

ANNUAL SUMMARY REPORT

P40: Installation of Ground Instrumentation (Sensor Arrays using Geophones and Accelerometers) for the Monitoring of Surface Response: Deception Bay Road (2017/2018)

ARRB Project No.: PRP16119

Author/s: Dr Jeffrey Lee and Dr Dominik Duschlbauer

Prepared for: Queensland Department of Transport and Main Roads

25/02/2020

01



AN INITIATIVE BY:

SUMMARY

In 2014, the Australian Road Research Board (ARRB) acquired a Traffic Speed Deflectometer (TSD) manufactured by Greenwood Engineering. It was then upgraded by ARRB, making it the first integrated road surface and sub-surface condition assessment system in the world. This device is known as the iPAVE system. Since then, the TSD has been conducting annual network surveys in Queensland, New South Wales, Western Australia and New Zealand.

The main aim of this NACoE project is to acquire a better understanding of TSD deflection data by installing ground instrumentation (i.e. sensor arrays using geophones and accelerometers) and monitoring the 'true' surface response when heavy vehicle traffic or other deflection testing devices travel over the pavement.

To complement the two deflection validation sites established in Western Australia, a permanent instrumentation site was established on Deception Bay Road (Road ID 121) in Queensland. The objective is to provide a high-quality site to monitor the pass-by of an iPAVE vehicle and allow a detailed and comprehensive comparison with FWD data.

Although the report is believed to be correct at the time of publication, the Australian Road Research Board, to the extent lawful, excludes all liability for loss (whether arising under contract, tort, statute or otherwise) arising from the contents of the report or from its use. Where such liability cannot be excluded, it is reduced to the full extent lawful. Without limiting the foregoing, people should apply their own skill and judgement when using the information contained in the report.

Presently, there are limited tools available in Australia to evaluate the deflection of a pavement as the iPAVE vehicle travels over a pavement. This research will provide invaluable data which will supplement the ground instrumentation site set up in Western Australia under the WARRIP research initiative.

This report provides details of the sensor selection and installation procedures used at the Deception Bay Roads site. Details of the iPAVE pass-by study will be reported in subsequent years; a more detailed analysis of the data will also be undertaken.

The project scope also includes an investigate study of the iPAVE data application. A technical note has been prepared to inform TMR districts of possible applications and potential risks associated with the iPAVE data usage.

Queensland Department of Transport and Main Roads Disclaimer

While every care has been taken in preparing this publication, the State of Queensland accepts no responsibility for decisions or actions taken <u>as a result of</u> any data, information, statement or advice, expressed or implied, contained within. To the best of our knowledge, the content was correct at the time of publishing.

ACKNOWLEDGEMENTS

TMR North Coast Region provided assistance with the identification of the ground instrumentation site on Deception Bay Road. Their help was very much appreciated by the project team.

CONTENTS

1	INTRODUCTION			
	1.1	BAC	(GROUND	1
	1.2	RECI	ENT WORK CONDUCTED IN WESTERN AUSTRALIA	2
2	SCC	PE OF	PROJECT	3
	2.1	RESE	EARCH AIM	3
3	MOE	DELS F	OR CONVERTING TSD DATA	4
	3.1	SPEC	CIFICS OF AUTC METHOD	5
4	SEN	SOR S	ELECTION AND INSTALLATION	6
	4.1	INTR	ODUCTION	6
	4.2	SITE	SELECTION	6
		4.2.1	SITE LOCALITY AND INFORMATION FROM ARMIS DATABASE	6
		4.2.2	GROUND INSTRUMENTATION SITE	8
	4.3	SENS	SOR SELECTION AND CALIBRATION	9
		4.3.1	SELECTION OF GEOPHONES	10
		4.3.2	SELECTION OF ACCELEROMETERS	10
		4.3.3	CALIBRATION OF SENSORS	12
	4.4	INST	ALLATION PROCEDURES	14
5	RESULTS AND DISCUSSION			
	5.1	FALL	ING WEIGHT DEFLECTOMETER (FWD)	17
6	CON	ICLUSI	ONS	22
RE	FERE	NCES.		23
ΑP	PEND	IX A	SLR CONSULTING REPORT – PERMANENT PAVEMENT INSTRUMENTATION	
			INSTALLATION	24
APPENDIX B		IX B	TMR DRAFT TECHNICAL NOTE	25

TABLES

Table 4.1:	Pavement condition and traffic data from ARIVIIS for Deception Bay Road	
Table 4.2:	Details of Sensors in Deception Bay Road	9
FIGUF	RES	
Figure 1.1	Photograph of Doppler laser in front of the rear dual-tyre axle	1
Figure 1.2	Geophone with protective cap installed	2
Figure 1.3	Comparison of selected deflection bowls from TSD and FWD (Left: Kwinana Freeway, Right: Leach Highway)	2
Figure 3.1	Pavement deflection velocity under a rolling load	4
Figure 3.2	Pavement deflection velocity and deflection bowl with deflection slopes (tangents)	4
Figure 4.1	Aerial photo showing the location of the ground instrumentation site	6
Figure 4.2	Pavement layers for the westbound left lane along Deception Bay Road	7
Figure 4.3	Photograph showing the condition of the pavement prior to installation of ground sensors	8
Figure 4.4	Sensor array geometry and sensor type	9
Figure 4.5	Sensor encapsulation schematic and photograph of a geophone used	10
Figure 4.6	Schematic and photograph of a capsule containing an accelerometer and a geophone	11
Figure 4.7	Schematic and photograph of an accelerometer only capsule	11
Figure 4.8	Photograph of laboratory shake table set up for calibrating each sensor	12
Figure 4.9	Calibration curve of a HG6-UB geophone	13
Figure 4.10	Calibration curve of a Wilcoxon piezoelectric IEPE 827T accelerometer	14
Figure 4.11	Installation photographs of the ground instrumentation array	15
Figure 5.1	FWD normalised maximum deflection at the instrumentation site	17
Figure 5.2	FWD normalised curvature function at the instrumentation site	18
Figure 5.3	FWD normalised deflection basin at the instrumentation site	18
Figure 5.4	Displacement measured at different offsets distance from the impact next to hole C	19
Figure 5.5	Displacement time histories from the impact next to hole C	19
Figure 5.6	Displacement measured at different offset distance from the impact next to hole F	
Figure 5.7	Displacement time histories from the impact next to hole F	
Figure 5.8	Typical measured time history of a FWD	21
Figure 5.9	Comparison of maximum deflection reported by a FWD and measured by the instrumentation array	21

1 INTRODUCTION

1.1 BACKGROUND

In 2014, the Australian Road Research Board (ARRB) acquired a Traffic Speed Deflectometer (TSD) manufactured by Greenwood Engineering. It was then upgraded by ARRB, making it the first integrated road surface and sub-surface condition assessment system in the world. This device is known as the iPAVE system. Since then, the TSD has been conducting annual network surveys in Queensland, New South Wales, Western Australia and New Zealand.

Several devices are available for pavement structural evaluation at the network level, including the ARA Rolling Wheel Deflectometer (RWD), Dynatest's RAPTOR™ Rolling Weight Deflectometer (RWD), and the Greenwood Engineering TSD.

In Australia, the TSD utilises Doppler lasers to measure the vertical surface velocity of the deflected pavement at six locations along the mid-line of the rear left dual tyres, directly under the rear axle and in front of the tyres at distances of 100, 200, 300, 600 and 900 mm from the rear axle. D_0 is defined as the deflection directly underneath the rear axle. The seventh Doppler laser, known as the reference laser, is positioned 3500 mm in front of the rear axle load. The reference laser is presumed to remain relatively unaffected by the load applied by the axles, whilst the vertical pavement deflection velocity of the reference laser is comparatively lower. Figure 1.1 shows a photograph of the different Doppler lasers located ahead of the rear dual-tyre axle.

Various deflection algorithms are available to compute pavement vertical surface deflection, including the Euler-Bernoulli beam model (Rasmussen et al. 2008), the ARRB 'Area Under the Curve' (AUTC) method (Austroads 2014; Muller & Roberts 2013), and the Weibull functional form method (Zofka et al. 2014).

Recent research conducted in the United States (Nasimifar et al. 2016) presented two methods, namely velocity-based and deflection-based approaches, to estimate the pavement layer moduli for network-level analysis using the TSD. The deflection-based approach, which is to back-calculate the layer moduli from TSD measured deflections, is being used to explore the use of TSD technology in pavement rehabilitation design in Queensland. This can be performed by first converting the TSD deflection velocity slope measurements to near equivalent FWD deflections. The software developed for the FWD is then employed to back-calculate layer moduli based on the TSD deflection measurements. This approach facilitates the use of TSD data with the already-established FWD back-calculation procedure.

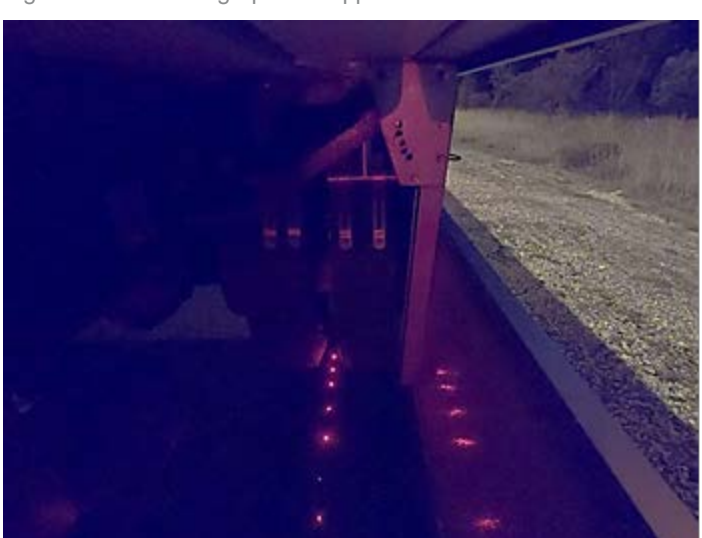


Figure 1.1 Photograph of Doppler laser in front of the rear dual-tyre axle

Source: Lee, Duschlbauer and Chai (2019).

1.2 RECENT WORK CONDUCTED IN WESTERN AUSTRALIA

In 2018, the project team (Main Roads Western Australia, ARRB and SLR Consulting Australia Pty Ltd (SLR)) designed and completed the installation of two ground-truth instrumentation sites near Perth (Kwinana Freeway and Leach Highway). The instrumentation sites (array of geophones, accelerometers and temperature sensors embedded near the pavement surface) were used to monitor the 'true' surface response when the deflection testing devices travelled over the sensor array. The primary objectives of the project were to:

- carry out a comparison of deflections made by the FWD and the TSD
- provide an independent tool to assess the FWD and TSD reported deflections
- gain a better understanding of TSD deflection data, in order to enhance the level confidence in the application of the technology.

A photograph of a geophone sensor used in the project is shown in Figure 1.2.

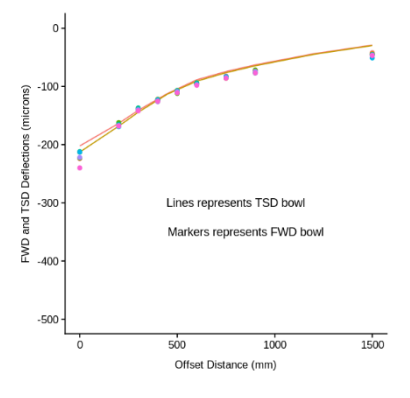
Figure 1.2 Geophone with protective cap installed

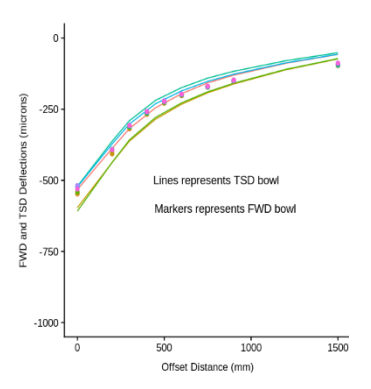


Source: Lee et al. (2019).

Figure 1.3 presents the deflection bowls measured with the embedded array while a TSD was passing over the array (lines) and for FWD impacts (markers). The results obtained with the embedded array showed good agreement with the results measured by the TSD and FWD. For the Kwinana Freeway site, there was a good match in the front end of the deflection bowl (0 to 600 mm). For the Leach Highway site, the deflection in the front end of the deflection bowl also had a good match between 0 mm to 900 mm offset. It was observed that the deflection profiles and correlation varied with pavement type.

Figure 1.3 Comparison of selected deflection bowls from TSD and FWD (Left: Kwinana Freeway, Right: Leach Highway)





Source: Lee et al. (2019).

2 SCOPE OF PROJECT

This is the third year (FY2017–18) of the NACoE project. The main task in FY2017–18 is to expand on the experimental plan tested in Year 2 (FY2015–16) and to conduct a 'ground-truth' experiment at a site on the TMR network. The scope includes the following tasks:

- Task 1: Refine project scope and expand the experimental plan tested in Year 2.
- Task 2: Conduct a 'ground-truth' experiment.
- Task 3: Analyse the data obtained from the experimental work.
- Task 4: Explore possible TSD applications.

2.1 RESEARCH AIM

Analytical models used to design and rehabilitate pavements are becoming increasingly sophisticated. The most appropriate process for verifying the accuracy and usefulness of these new analytical models (a well as for calibrating the parameters included in these models) is to observe the response behaviour of pavements in the field. One economical alternative is to use velocity transducers (geophones) to determine the displacement of a pavement section under actual loads. If used correctly, geophones can provide quite accurate deflection-time history data (Nazarian & Bush 1989).

The main aim of this project is to acquire a better understanding of TSD deflection data by installing ground instrumentation (i.e. sensor arrays using geophones and accelerometers) and monitoring the 'true' surface response when heavy vehicle traffic or other deflection testing devices travelled over the pavement. To complement the two deflection validation sites established in Western Australia, a permanent instrumentation site on Deception Bay Road (Road ID 121) was established under the NACoE project in Queensland. Details of the sensor selections and installation procedures are detailed in this report.

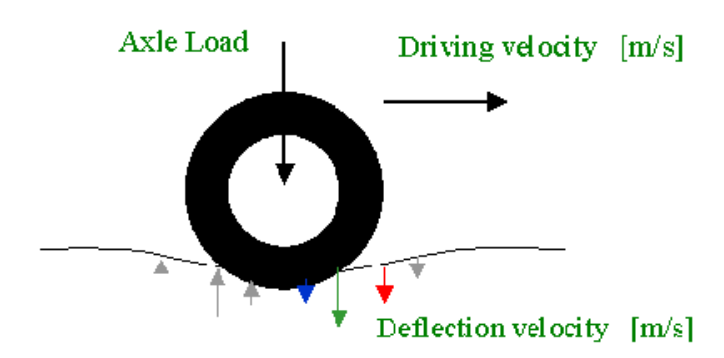
3 MODELS FOR CONVERTING TSD DATA

The TSD measures the vertical velocity of the pavement surface while traveling at traffic speed (nominally 80 km/h). A deflection bowl is obtained by integrating the velocity slopes from each of the Doppler lasers. Parameters such as maximum deflection, curvature, and other structural condition indices can then be derived from the deflection bowl. Two methods are available for converting TSD deflection velocity slope to deflection:

- Euler-Bernoulli beam model (Rasmussen et al. 2008), more commonly known as the 'Greenwood Model'
- ARRB 'area under the curve' (AUTC) method (Muller & Roberts 2013).

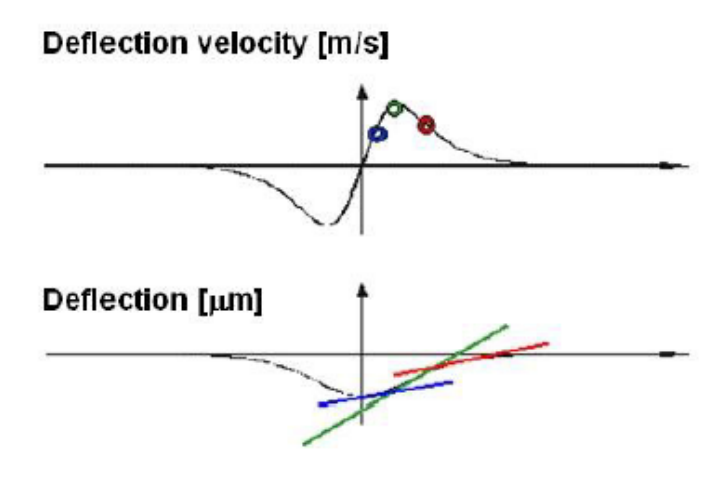
During operations, the Doppler sensors measure vertical velocities of the deflected pavement surface at discrete points and, when divided by the instantaneous vehicle speed, velocity slopes (V_v/V_h) at those points can be calculated (Rasmussen et al. 2008). Figure 3.1 shows the pavement deflection velocity vectors under a rolling wheel. Together with the deflection velocity, the corresponding deflection bowl is shown in Figure 3.2, where deflection slopes (tangents) are displayed. The pavement deflections can be determined by integrating the deflection slope curve using a closed-form solution of a mechanical model such as an elastic beam on a Winkler foundation (Rasmussen et al. 2008).

Figure 3.1 Pavement deflection velocity under a rolling load



Source: Rasmussen et al. (2008).

Figure 3.2 Pavement deflection velocity and deflection bowl with deflection slopes (tangents)



Source: Rasmussen et al. (2008).

The current algorithm being used by the manufacturer is based on a statistical method that fits a curve through the TSD data (Pedersen 2013); it also accounts for asymmetry in the deflection bowl (Nasimifar et al. 2016).

3.1 SPECIFICS OF AUTC METHOD

The AUTC method was first developed following the initial TSD trials conducted in Australia in 2010 (Muller & Roberts 2013). The method involves fitting the TSD slope measurements and numerically integrating them over the length of the deflection bowl, working towards the wheel load. Details are as follows:

- The base TSD data consists of a set of vertical pavement velocities, referenced against horizontal offsets spaced along the axis of the wheelpath and away from the loading of the dual-tyred truck wheels. This data is termed the velocity profile.
- The value of the velocity at each point is a function of the pavement strength, the offset of the Doppler laser (i.e. the velocity sensor) from the centre point of loading, and the horizontal speed of the TSD (which affects the speed of the vertical loading).
- The slope is the ratio between the vertical and horizontal velocities at each measurement point and the
 actual physical slope of the pavement surface within the deflection bowl centred under the moving TSD's
 rear wheel.
- By plotting slope values against the offsets from the load point as a slope profile curve (analogous to the
 previously-mentioned velocity profile), it is possible to show that the cumulative area under the slope
 profile working from the tail adds up to the vertical deflection at that point where the load is applied.
- The vertical difference between any two deflection points, such as for the bowl curvature, (D_0-D_{200}) , is equal to the area under the slope profile curve between these two points.

4 SENSOR SELECTION AND INSTALLATION

4.1 INTRODUCTION

SLR was engaged by ARRB to assist with the permanent installation of instrumentation arrays on Deception Bay Road, north of Brisbane, Queensland. A report presenting the methodology and the installation details was prepared by SLR (see Appendix A).

4.2 SITE SELECTION

4.2.1 SITE LOCALITY AND INFORMATION FROM ARMIS DATABASE

Figure 4.1 shows an aerial photo of the site. It is located near Chainage 5.91 km along the westbound (anti-gazettal) left lane of the Deception Bay Road (121).

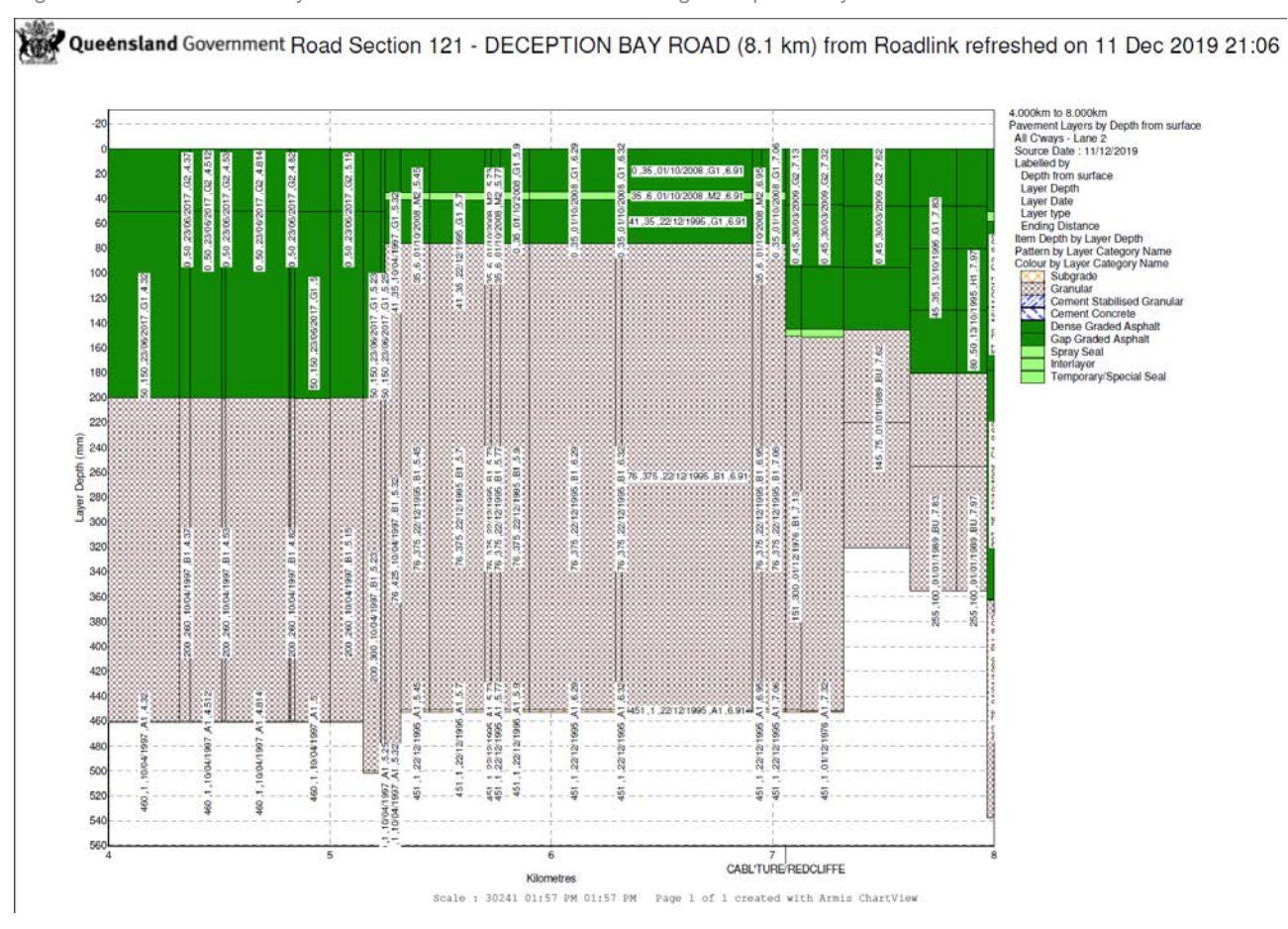
Figure 4.1 Aerial photo showing the location of the ground instrumentation site



Source: nearmap 2019, 'Deception Bay, Queensland, nearmap image', viewed on 10 December 2019, https://apps.nearmap.com/maps/#/@-27.2015230,153.0348925,20.00z,0d/V+R/20191106.

Figure 4.2 is an extract from the TMR ARMIS database showing the layers of the pavement where the ground instrumentation site was installed. The pavement comprises 70 mm of asphalt over 375 mm of unbound granular pavement. The pavement construction was consistent and the pavement was in good condition. No pavement surface maintenance work was scheduled.

Figure 4.2 Pavement layers for the westbound left lane along Deception Bay Road



The Deception Bay Road is an arterial road located about 40 km north of the Brisbane CBD. Details of the surface characteristics are summarised in Table 4.1. A photograph showing the site condition prior to the installation of the ground instrumentation sensors is depicted in Figure 4.3. The arterial road consists of a two lanes per carriage configuration along a straight and level section.

Table 4.1: Pavement condition and traffic data from ARMIS for Deception Bay Road

Property		
Surfacing type	Dense-graded asphalt	
Carriageway AADT (2018)	13 864 vehicles/carriageway/day	
Posted speed	70 km/h	
Percentage heavy vehicles (%)	3	
TSD deflection D ₀ (2017)	273.5 microns	
NAASRA roughness count (counts/km) (2018)	44	
Rutting (mm) (2018)	5.6	
Texture depth (mm)	0.56	
Cracking – all (2018)	8%	
Pavement configuration	35 mm asphalt surfacing 35 mm asphalt binder layer 375 mm granular base Subgrade	

Figure 4.3 Photograph showing the condition of the pavement prior to installation of ground sensors

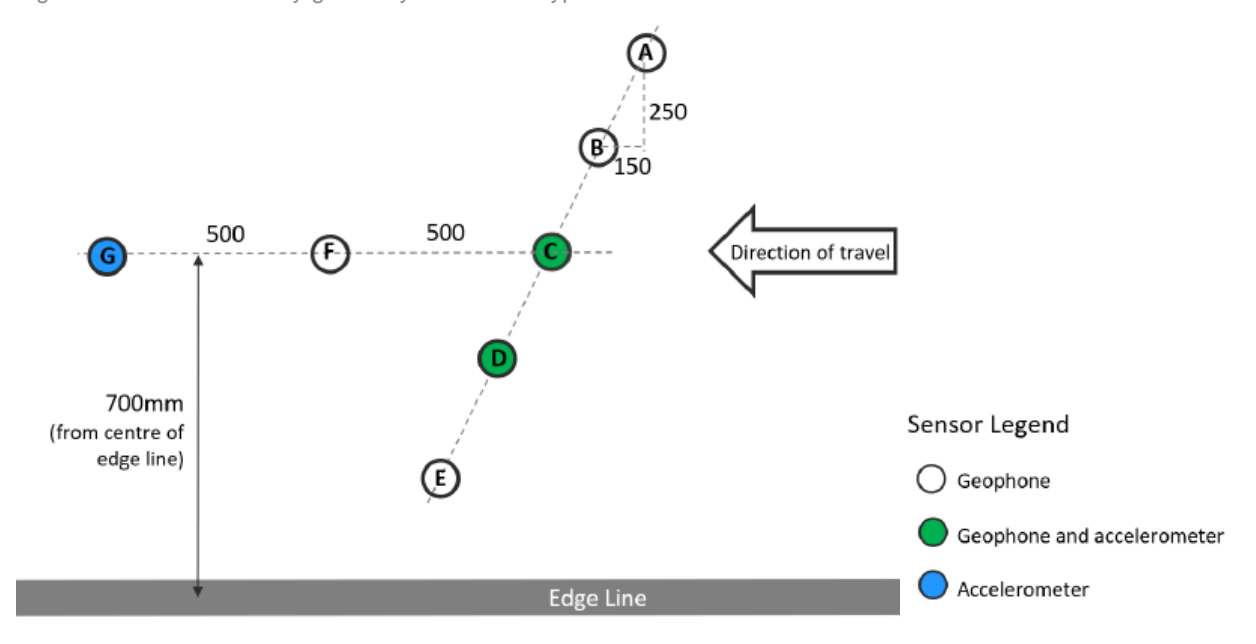


4.2.2 GROUND INSTRUMENTATION SITE

Both geophones (measuring velocities) and accelerometers (measuring accelerations) were installed at the site on the nights between 1 and 3 October 2019, and a schematic diagram of the instrumentation array is shown in Figure 4.4. Based on previous experience of similar instrumentation sites in Western Australia, the sensor array was strategically designed to minimise the effect of the wandering of the iPAVE as it travels past the sensor array. The array extends \pm 250 mm laterally from the wheelpath and 1000 mm in the longitudinal direction.

Single geophones were installed in Holes A, B, E and F. Holes C and D accommodated both geophones and accelerometers, which are designed to validate the accuracy of the measurement of both sensors. Hole G has a single high-precision accelerometer located 1000 mm away from Hole C. It is used to provide a high accuracy acceleration history and also for the determination of the instantaneous speed of the iPAVE when it travels past the array.

Figure 4.4 Sensor array geometry and sensor type



4.3 SENSOR SELECTION AND CALIBRATION

Both geophones (velocity sensor) and accelerometers (acceleration sensor) were used during the installation. The sensors were selected carefully for their performance and long-term stability in an exterior environment. Details of the sensors and the installation depths are summarised in Table 4.2. After the installation of the sensors, polyurethane resin (PU200) was poured into the drilled holes.

Table 4.2: Details of Sensors in Deception Bay Road

Drilled hole designation	Sensor type	Manufacturer and sensor model number	The diameter of drilled hole (mm)	Depth of drilled hole (mm)
A	Geophone	HGS HG6-UB	72	70
В	Geophone	HGS HG6-UB	72	70
С	Geophone	HGS HG6-UB	72	90
	Accelerometer	Dytran 3305A3		
D	Geophone	HGS HG6-UB	72	90
	Accelerometer	Dytran 3305A3		
E	Geophone	HGS HG6-UB	72	70
F	Geophone	HGS HG6-UB	72	70
G	Accelerometer	Wilcoxon 728T	72	70

The monitoring of long-term pavement performance (LTPP) is being conducted by many road agencies worldwide. One of the methods used in LTPP studies is to measure the deflections with displacement probes embedded in the pavement and the displacement of the pavement relative to their anchor points. The installation of displacement probes is comparatively difficult. This is because, contrary to the displacement probes, geophones and accelerometers measure absolute quantities, which does not require a datum to be established in the field. The practical implications are that small sensors can be deployed in the upper layers of the pavement, minimising the impact in terms of installation efforts. This is the main attractive feature of the method.

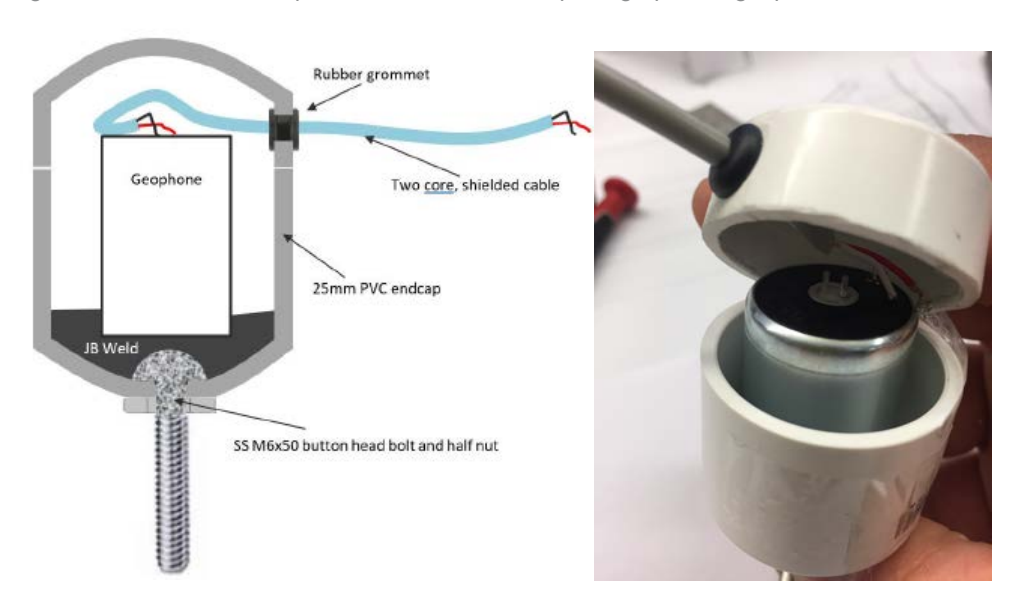
4.3.1 SELECTION OF GEOPHONES

Geophones were selected as the main sensor for this project because:

- · worldwide, geophones have been successfully used to effectively to monitor deflections in a pavement
- they are robust sensors and pavement deflections can be obtained via a single integration step
- the FWD uses geophones as well
- good experience gained from the geophone installation in Perth.

The geophones deployed on Deception Bay Road have a nominal sensitivity of 30 (Volts per m/s) and a resonant frequency of 4.5 Hz. Each geophone was sealed inside a PVC casing and individually calibrated in the laboratory to establish the calibration curve over the frequency range (refer to Figure 4.5).

Figure 4.5 Sensor encapsulation schematic and photograph of a geophone used



4.3.2 SELECTION OF ACCELEROMETERS

Accelerometers measure the vertical acceleration of the pavement surface. By double-integrating the measured acceleration time history, deflection (or displacement) profiles can be determined.

Modern accelerometers can be very small (similar to the one used in this project) and they are able to withstand high G-forces. In addition, it is possible to select accelerometer models with a frequency response (i.e. the sensitivity as a function of frequency) that is almost constant over the frequency range of interest.

For this project, two types of accelerometers were used:

- Dytran 3305A3 (500 mV/g)
- Wilcoxon 728T (500 mV/g).

The Dytran accelerometers have very small dimensions; they were encapsulated with geophones as one unit (refer to Figure 4.6). The Wilcoxon accelerometer, due to its larger size, was encapsulated individually (refer to Figure 4.7).

Figure 4.6 Schematic and photograph of a capsule containing an accelerometer and a geophone

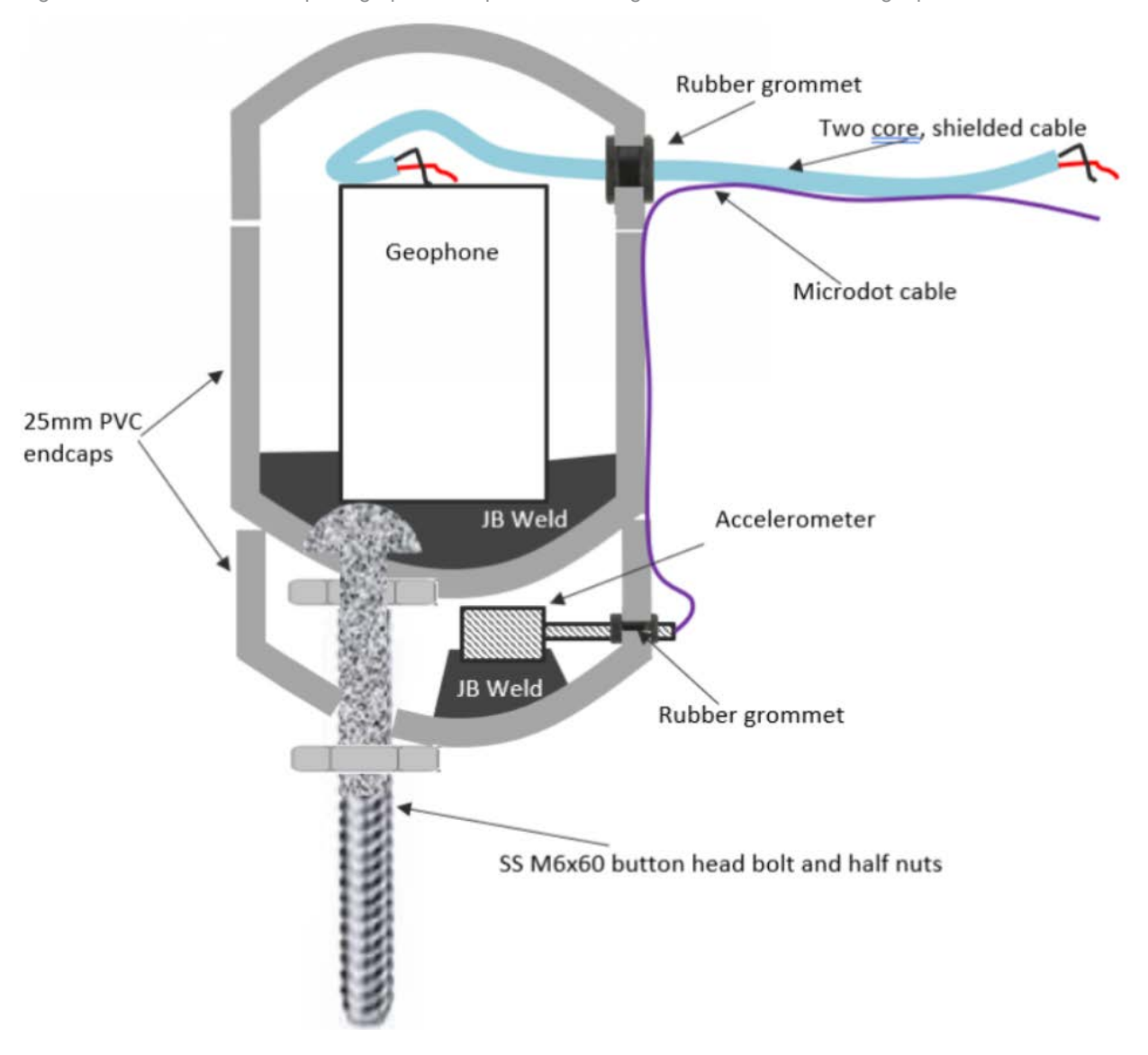
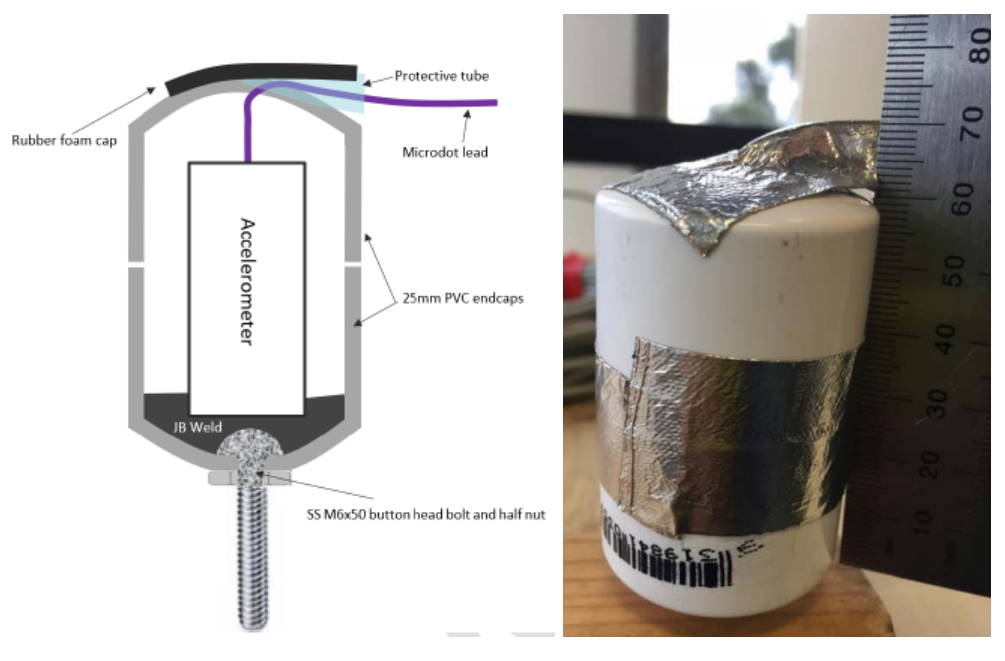


Figure 4.7 Schematic and photograph of an accelerometer only capsule



4.3.3 CALIBRATION OF SENSORS

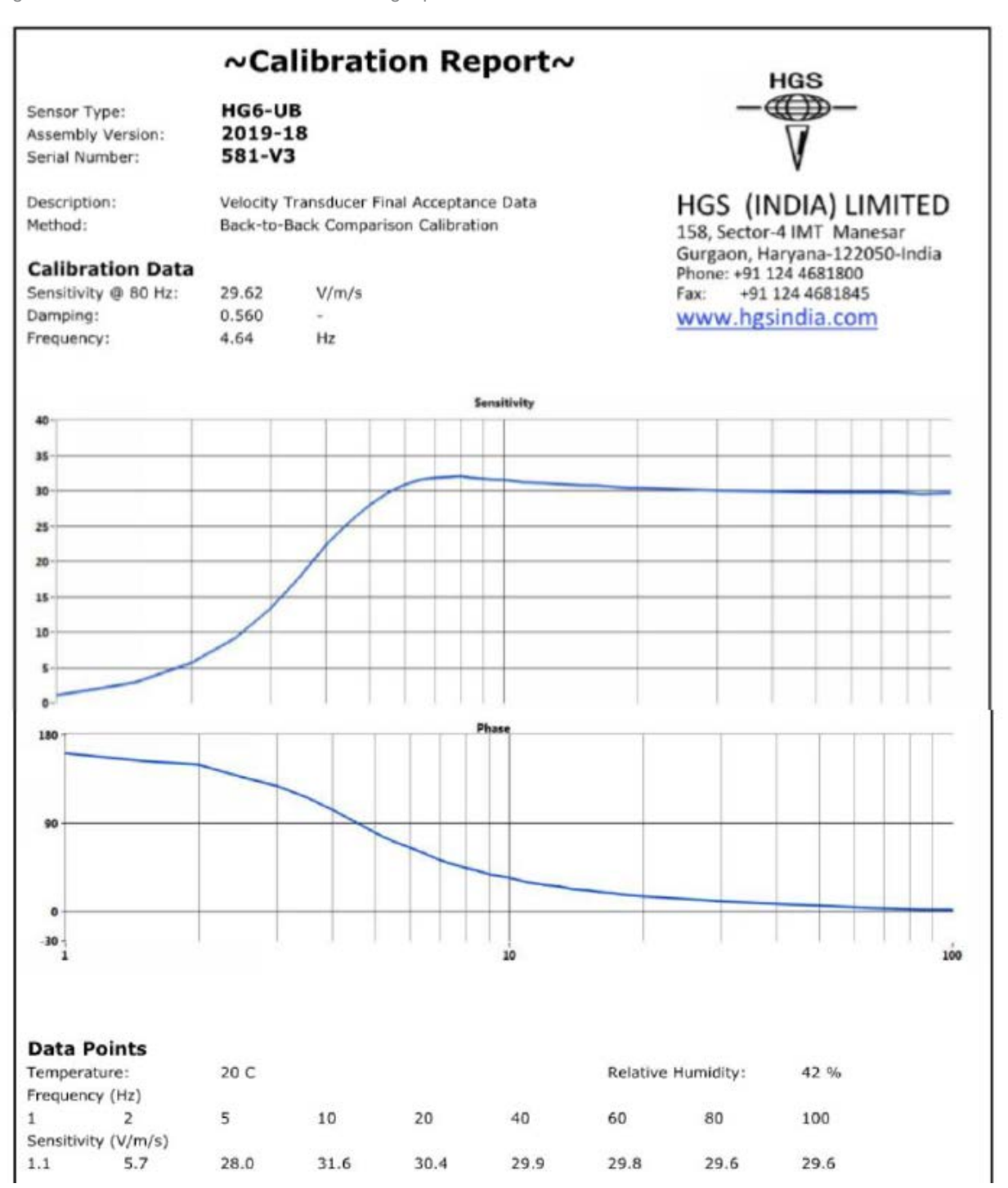
The calibration of the sensors was conducted using the in-house dynamic shaker in the Lane Cove office of SLR Consulting (Figure 4.8). The process involved placing each encapsulated sensor (geophone or accelerometer) and a reference sensor on the dynamic shaker table. Then, a waveform generator was used to drive the dynamic shaker using a range of waveforms (i.e. sweeping sinusoidal waveform from low to high frequencies). The output from the sensor was then compared with the reference sensor to establish the calibration factor for each frequency range (calibration curve). The results were then compared with the factory calibration curves from the geophone and accelerometer manufacturer (Figure 4.9 and Figure 4.10, respectively).

Figure 4.8 Photograph of laboratory shake table set up for calibrating each sensor





Figure 4.9 Calibration curve of a HG6-UB geophone





Calibration Data

General Purpose Accelerometer

	Model 728T	Serial Number 5378
Sensitivity	503 mV/g	51.3 mV/m/s²
Bias Voltage	9.8 Vdc	
Resonance	20.0 kHz	1198.08 kcpm
Maximum Amplitude Range	15 g peak	147 m/s² pk
Transverse Sensitivity	1 %	
Frequency Response		
±5%:	2.0 Hz to 5.8 kH	z 120 cpm to 348 kcpm
±10%:	1.2 Hz to 10.7 k	Hz 72 cpm to 640 kcpm
±3dB:	0.8 Hz to kHz	48 cpm to
Calibrated by	T.PHOUBANDIT	H Date: 07/12/2019

This calibration is traceable to the National Institute of Standards and Technology, Gaithersburg, MD 20899.

Frequency Response is traceable 5 Hz to 10 kHz.

Sensitivity measured at 100 Hz, 1g, 25°C.

Low end frequency response and amplitude range are nominal values.

4.4 INSTALLATION PROCEDURES

The installation of the geophones and accelerometers was carried out over three (3) consecutive nights, between 1–3 October 2019. On the first two nights, civil works such as the installation of the cable pit and the field cabinet was undertaken. On the third night, the ARRB team directed the saw-cutting crew and installed the ground instrumentation sensors. This was followed by testing the integrity and operational readiness of the sensors using an instrumented impact hammer. An instrumented impact hammer features a rugged, force load cell that is integrated into the hammer's striking surface. All measurements were conducted using a portable HBM data acquisition system, and analysed off-site. Photographs taken during the installation are shown in Figure 4.11.

Figure 4.11 Installation photographs of the ground instrumentation array



Telecommunication field cabinet



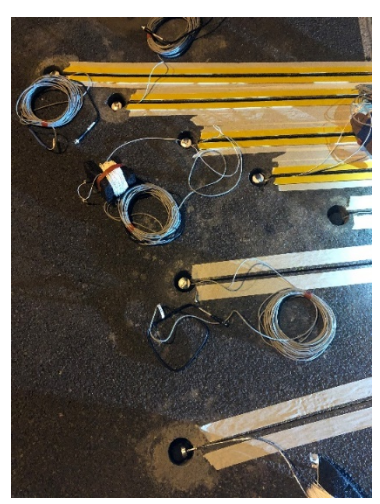
Saw cut for wire to run from sensor to cable pit



PVC conduit from the kerb into the cable pit



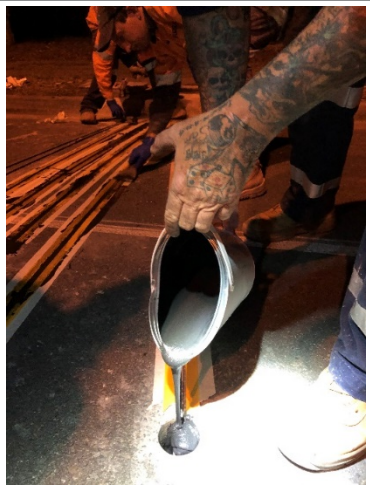
Coring on the pavement surface prior to sensor installation



Sensors installed in core holes



Running cables to the telecommunication field cabinet



Pouring of polyurethane resin sealant



Completion of sensor installation and carrying out of instrumented hammer testing to confirm operation of sensors

5 RESULTS AND DISCUSSION

As already discussed, the scope of the project in FY2019-20 was to install the ground instrumentation sensors and demonstrate their operational readiness. In the subsequent year, iPAVE testing will be conducted at the site. The results obtained from the iPAVE, FWD and the ground instrumentation sensors will then be assessed and compared.

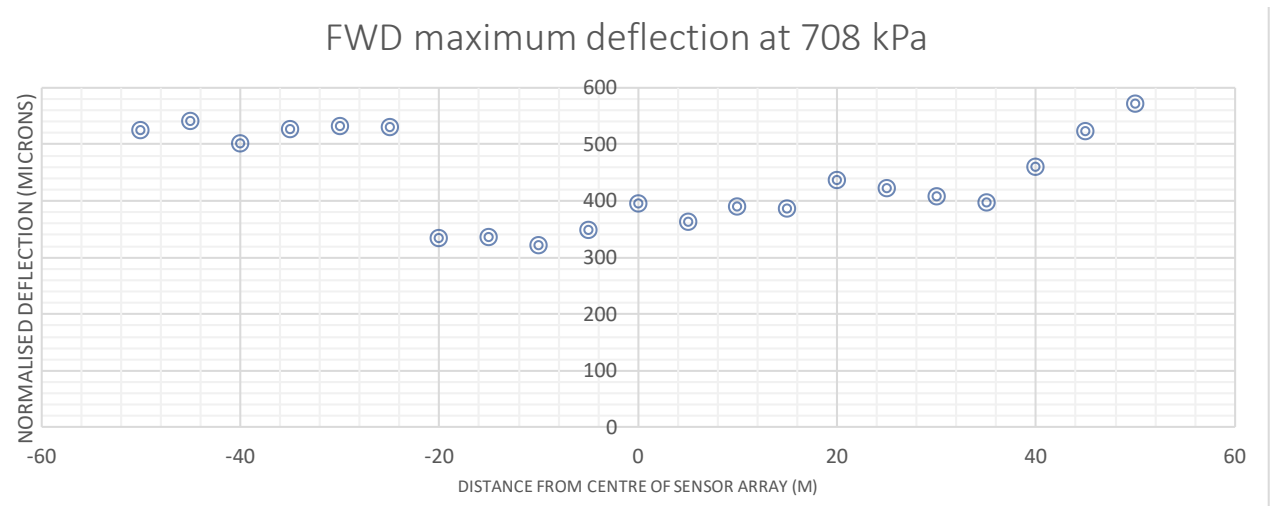
In this section, the collected FWD data are presented to confirm that:

- the site is uniform (in terms of maximum deflection and curvature)
- the sensors are all operational and providing comparable measurements of displacement.

5.1 FALLING WEIGHT DEFLECTOMETER (FWD)

FWD deflection testing was conducted with a target load of 50 kN (normalised to 708 kPa). The normalised maximum deflection (D_0) and normalised curvature (D_0 – D_{200}) collected on-site are shown in Figure 5.1 and Figure 5.2 respectively. It can be seen that the pavement deflection was consistent 20 m before and after the location of the sensor array. The normalised deflection bowl for the same area is shown in Figure 5.3. The magnitude and shape of the bowl aligns with the typical pavement performance of the pavement structure reported in ARMIS.

Figure 5.1 FWD normalised maximum deflection at the instrumentation site



Note: Air temperature of 24 °C and pavement surface temperature of 32 °C.

Figure 5.2 FWD normalised curvature function at the instrumentation site

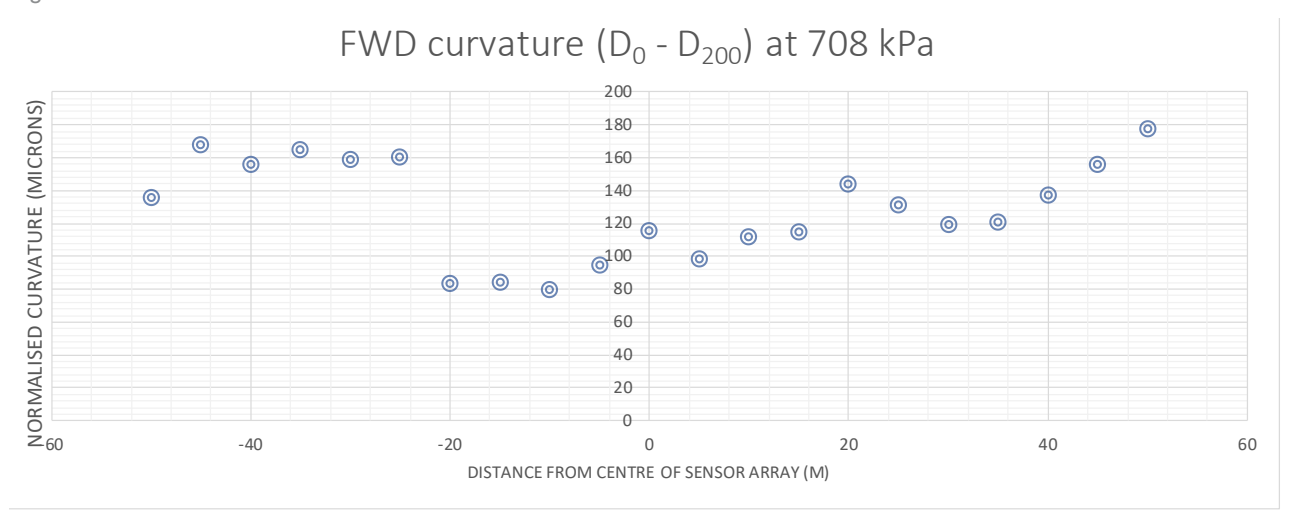
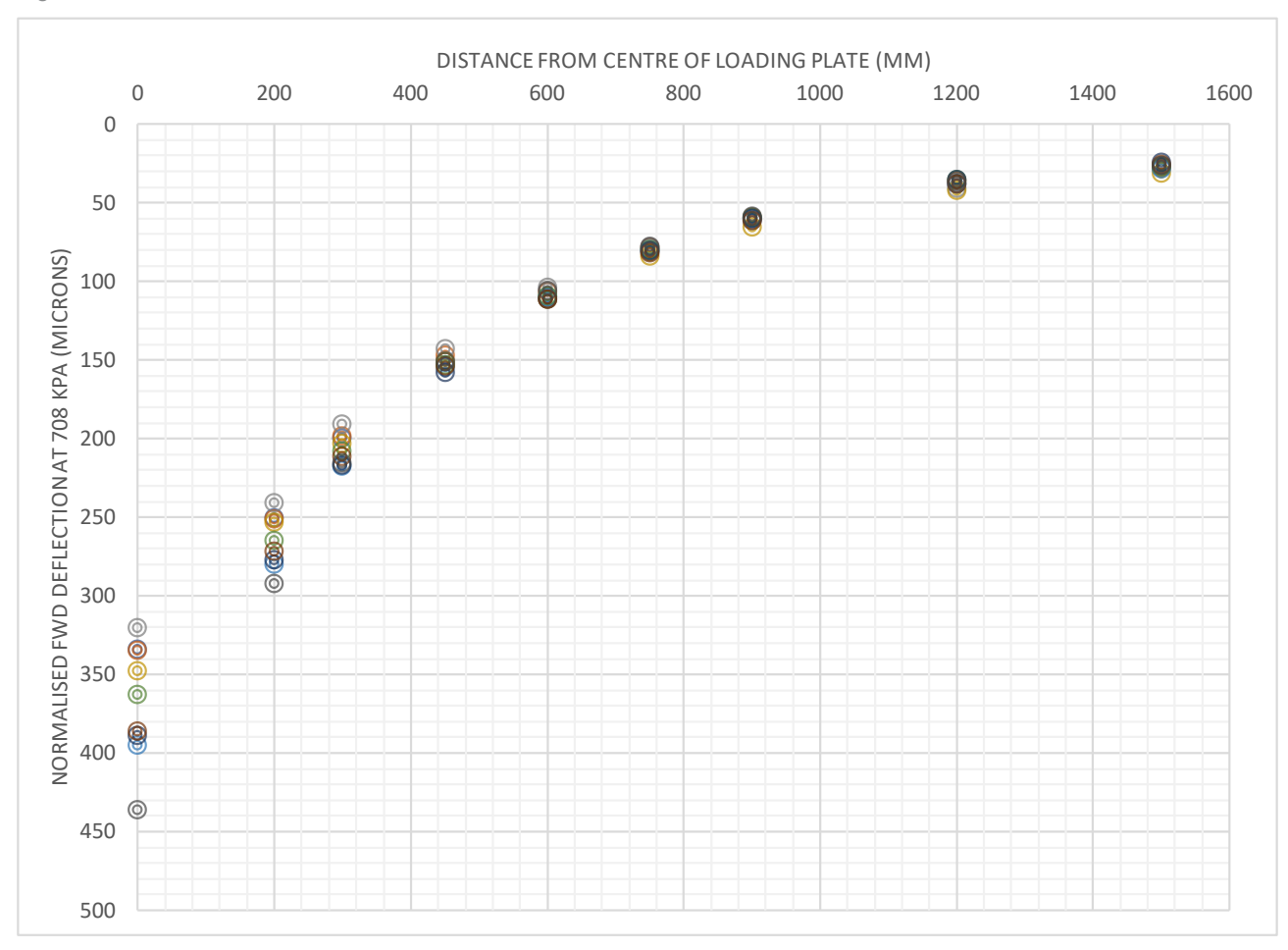


Figure 5.3 FWD normalised deflection basin at the instrumentation site



Shortly after the installation and the curing of the polyurethane resin, the ARRB team conducted a number of instrumented impact hammer tests at or near each of the sensors to confirm the operational readiness. The results from the direct hits are shown in Figure 5.4 to Figure 5.7. These impact tests were designed to provide a quick check to confirm the integrity of all cabling connections.

Figure 5.4 Displacement measured at different offsets distance from the impact next to hole C

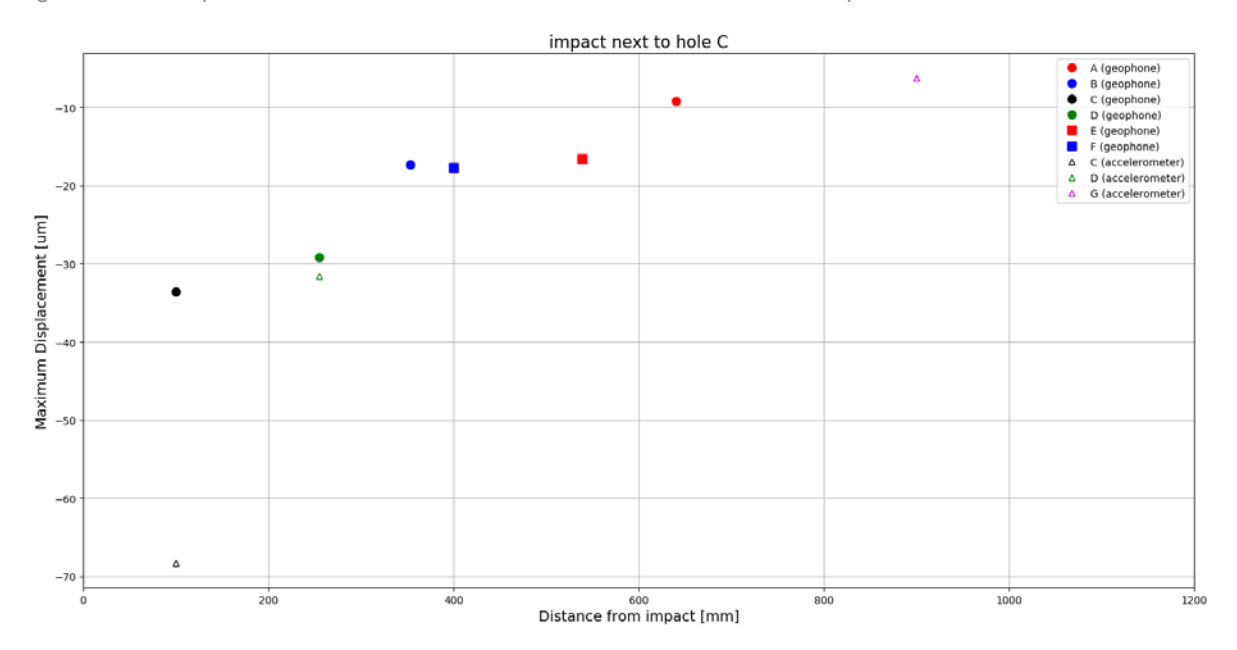


Figure 5.5 Displacement time histories from the impact next to hole C

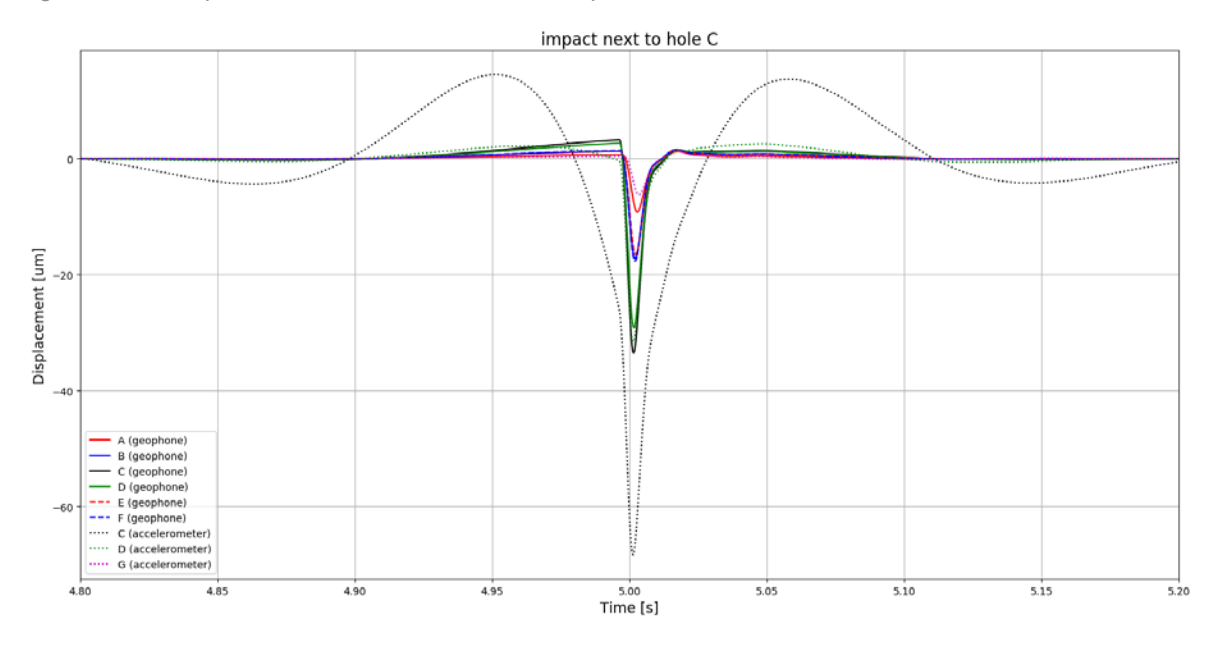


Figure 5.6 Displacement measured at different offset distance from the impact next to hole F

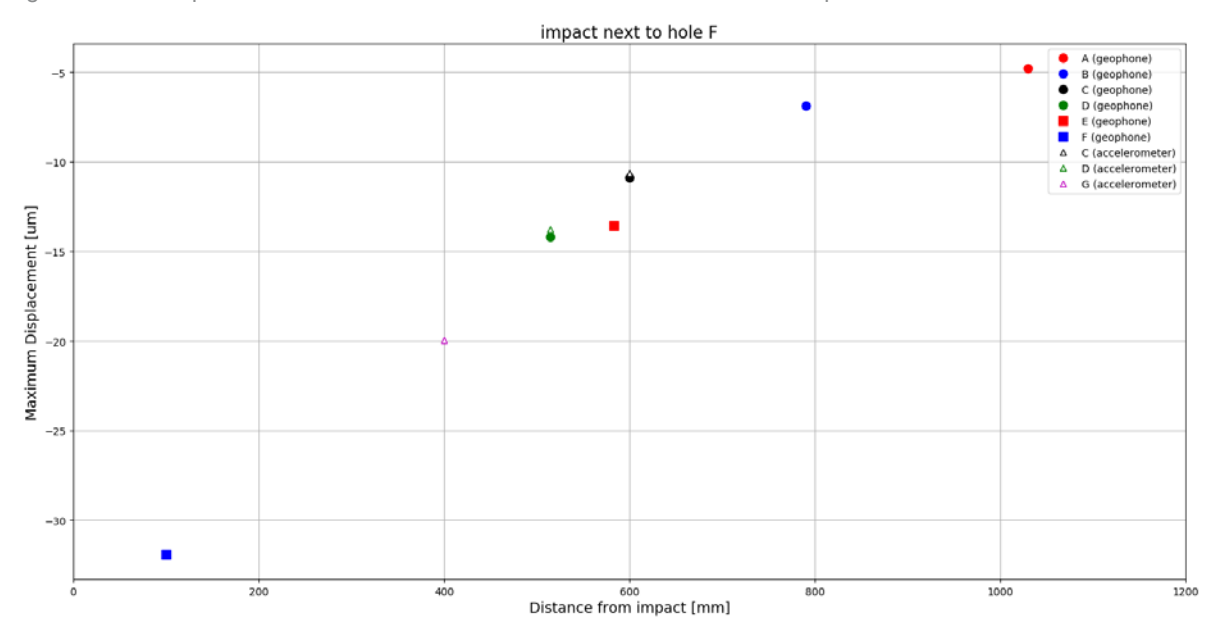
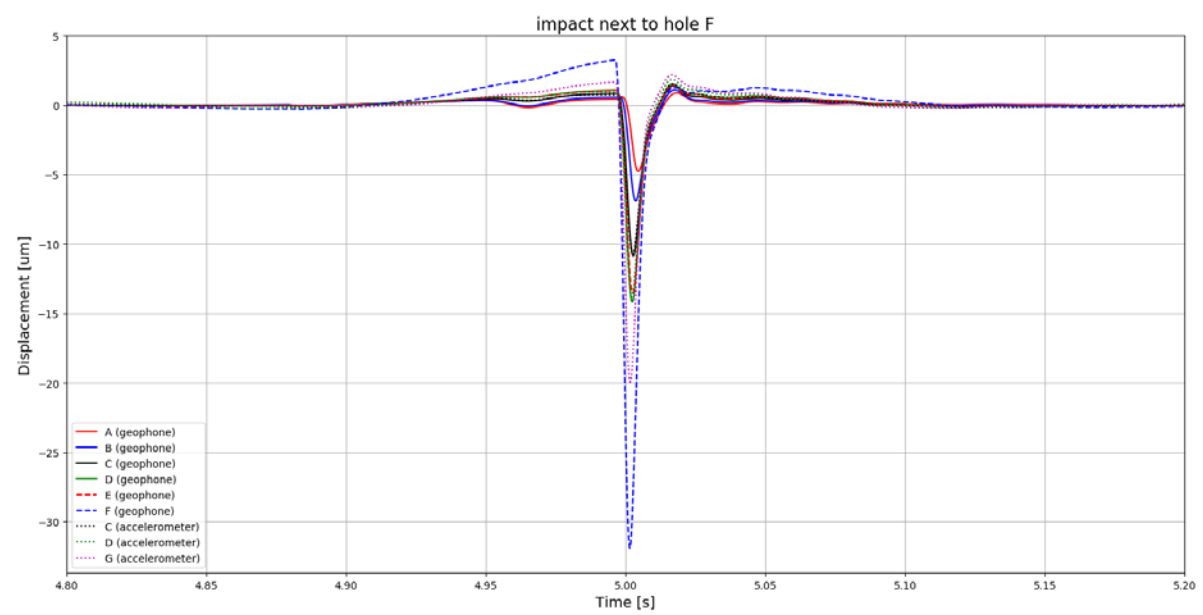


Figure 5.7 Displacement time histories from the impact next to hole F



The last step in validating the sensor installation was to compare the measured response from each hole to the FWD deflections. Figure 5.8 is a time history measured after an FWD impact drop. The time history signature is typical for FWDs as it clearly shows the decay impacts of the falling weight as it bounces and comes to a standstill. For the FWD impacts, it was found that the peak displacement could be interpreted in two ways: (i) absolute, i.e. the maximum displacement from zero (Figure 5.8, red arrow), or (ii) relative – i.e. the maximum peak-to-peak displacement (Figure 5.8, blue arrow). Generally, the relative displacements were found to be typically 10% greater than the absolute displacements; and the peak-to-peak (i.e. relative) displacements were found to have a better fit with the FWD reported deflections (Figure 5.9).

Figure 5.8 Typical measured time history of a FWD

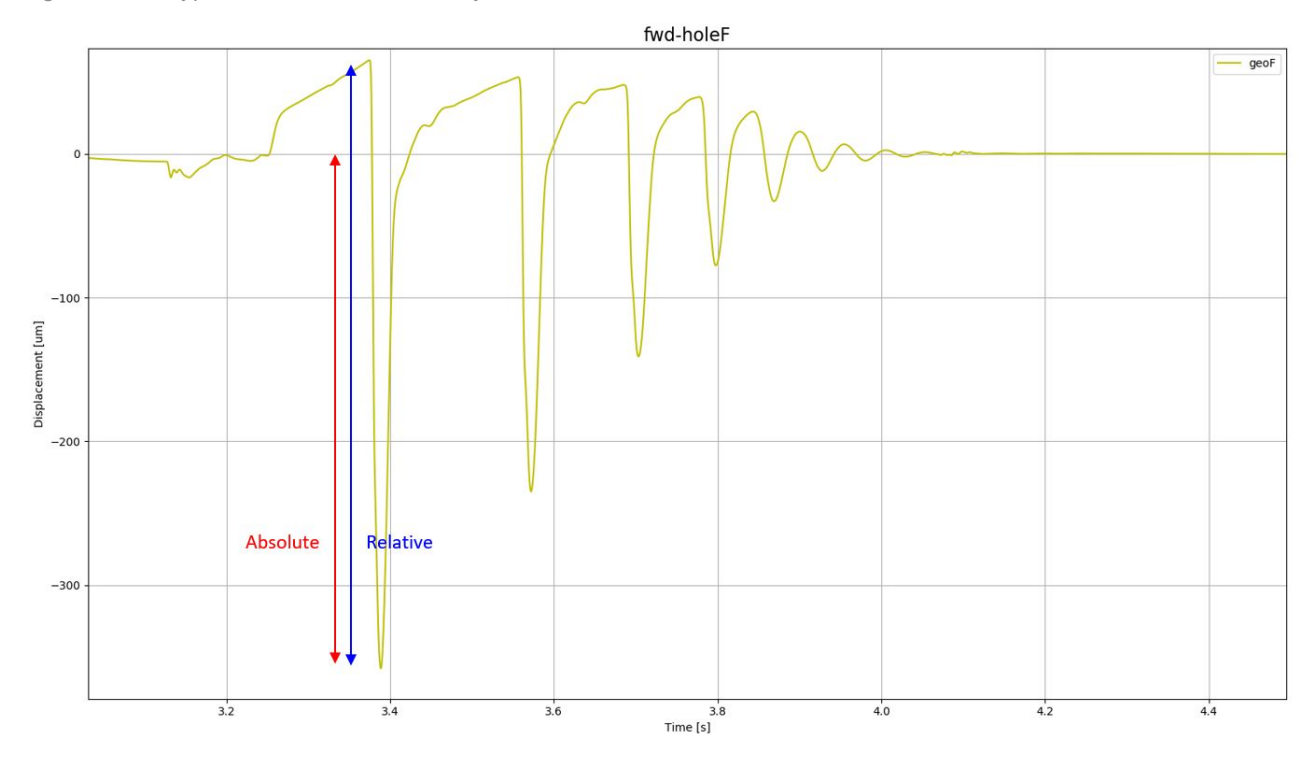
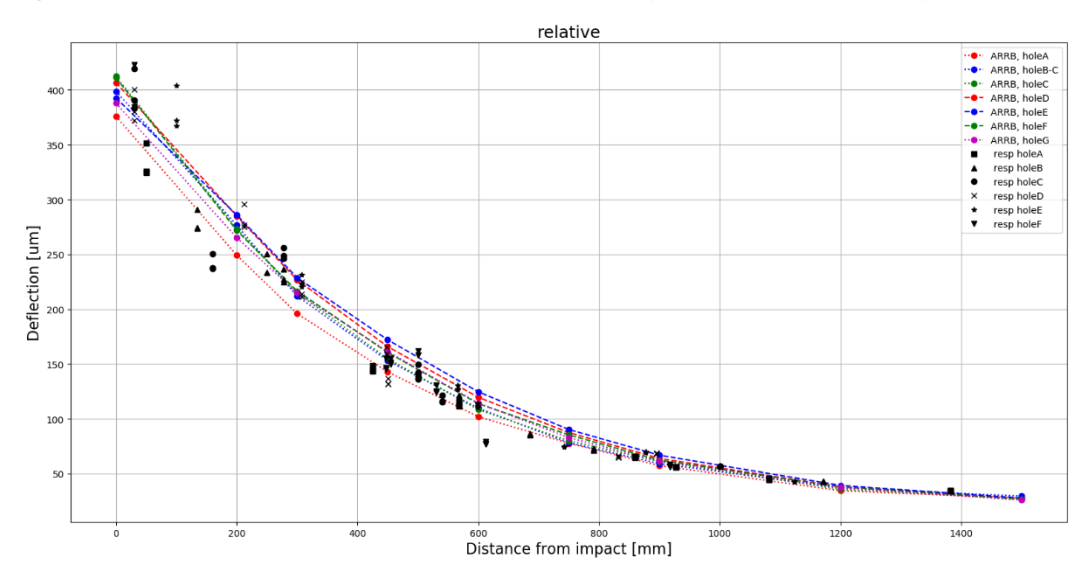


Figure 5.9 Comparison of maximum deflection reported by a FWD and measured by the instrumentation array



6 CONCLUSIONS

The project scope for this NACoE project in the current financial year was to install a ground instrumentation site and to investigate the application of the iPAVE data. A technical note has been prepared to inform TMR Districts of possible applications and the limitations associated with the iPAVE data usage. Presently, there are limited tools available in Australia to evaluate the deflection of a pavement as the iPAVE vehicle travels over a pavement. This research will provide invaluable data which will supplement a similar ground instrumentation site setup in Western Australia under the WARRIP research initiative.

A ground instrumentation site has been set up on Deception Bay Road near Brisbane. The objective is to provide a high-quality site to monitor the pass-by of an iPAVE vehicle and allow a detailed and comprehensive comparison with FWD data. This report only covers the methodology for installation and validation of the sensors. Details of the iPAVE pass-by study will be reported in subsequent years; a more detailed analysis of the data will also be undertaken.

REFERENCES

- Austroads 2014, *Traffic speed deflectometer data review and lessons learnt*, by J Roberts, U Ai, T Toole & T Martin, AP-T279-14, Austroads, Sydney, NSW.
- Lee, J, Duschlbauer, D & Chai, G 2019, *Ground Instrumentation for Traffic Speed Deflectometer*, report 2018-002, Western Australian Road Research and Innovation Program (WARRIP), Perth, Australia.
- Muller, WB & Roberts, J 2013, 'Revised approach to assessing Traffic Speed Deflectometer data and field validation of deflection bowl predictions', *International Journal of Pavement Engineering*, vol. 14, no. 4, pp. 388-402.
- Nasimifar, M, Thyagarajan, S, Siddharthan, RV & Sivaneswaran, N 2016, 'Robust deflection indices from traffic-speed deflectometer measurement to predict critical pavement responses for network-level pavement management system application', *Journal of Transportation Engineering*, vol. 142, no. 3, pp. 11.
- Nazarian, S & Bush, A, 1989, 'Determination of deflection of pavement systems using velocity transducers', *Transportation Research Record*, 1227, pp. 147-58.
- Pedersen, L 2013, 'Viscoelastic modelling of road deflections for use with the Traffic Speed Deflectometer', PhD thesis, Department of Mathematics, Technical University of Denmark.
- Rasmussen S, Aagaard, L, Baltzer, S & Krarup, J 2008, 'A comparison of two years of network level measurements with the Traffic Speed Deflectometer', *Transport Research Arena Europe*, 2008, *Ljubljana*, 8pp.
- Zofka, A, Sudyka, J, Maliszewski, M, Harasim, P & Sybilski, D 2014, 'Alternative approach for interpreting Traffic Speed Deflectometer results', *Transportation Research Record*, no. 2457, pp. 12-18.

APPENDIX A SLR CONSULTING REPORT – PERMANENT PAVEMENT INSTRUMENTATION INSTALLATION

PERMANENT PAVEMENT INSTRUMENTATION

Installation Deception Bay, QLD

Prepared for:

ARRB 21 McLachlan St, Fortitude Valley, QLD 4006





PREPARED BY

SLR Consulting Australia Pty Ltd
ABN 29 001 584 612
Grd Floor, 2 Lincoln Street
Lane Cove NSW 2066 Australia
(PO Box 176 Lane Cove NSW 1595 Australia)
T: +61 2 9427 8100
E: sydney@slrconsulting.com www.slrconsulting.com

BASIS OF REPORT

This report has been prepared by SLR Consulting Australia Pty Ltd (SLR) with all reasonable skill, care and diligence, and taking account of the timescale and resources allocated to it by agreement with ARRB (the Client). Information reported herein is based on the interpretation of data collected, which has been accepted in good faith as being accurate and valid.

This report is for the exclusive use of the Client. No warranties or guarantees are expressed or should be inferred by any third parties. This report may not be relied upon by other parties without written consent from SLR.

SLR disclaims any responsibility to the Client and others in respect of any matters outside the agreed scope of the work.

DOCUMENT CONTROL

Reference	Date	Prepared	Checked	Authorised
610.18975-R01-v0.1	11 October 2019	Dominik Duschlbauer	Aaron Miller	Draft



Deception Bay Road, Deception Bay, QLD

CONTENTS

1	INTRODUCTION	4
2	ARRAY LOCATION AND GEOMETRY	4
3	CONCLUSIONS	8
DOCUM	AFAIT DEFEDENCES	
DOCUN	MENT REFERENCES	
TABLES		
Table 1	Instrumentation	6
FIGURES		
Figure 1	Approximate location of the pavement array (red) and wayside cabinet	
	(yellow)	4
Figure 2	Sensor array	5
Figure 3	Array geometry and sensor type	
Figure 4	Geophone only encapsulation schematic	
Figure 5	Geophone only sensor preparation photos	
Figure 6	Combined geophone and accelerometer encapsulation schematic	
Figure 7	Combined geophone and accelerometer preparation photos	13
Figure 8	Accelerometer only encapsulation schematic (left) and closed capsule without	
	the rubber cap and protective tube (right).	14

APPENDICES

Appendix A Sensor Encapsulation Appendix B Sensor Sensitivities



1 Introduction

SLR Consulting Australia Pty Ltd (SLR) was engaged by The Australian Road Research Board (ARRB) to assist with the permanent installation of a sensor array in a pavement on Deception Bay Road, Deception Bay, QLD.

This report provides an overview of the installation and the instrumentation deployed.

2 Array Location and Geometry

The pavement sensors were installed on the night of Thursday 3 October to Friday 4 October 2019. This was the third night of a program lasting for three nights (from 1 October to 3 October) with a wayside cabinet and cable pit being installed on nights 1 and 2.

The array's sensors are clustered around GPS coordinates (-27.200704, 153.03379)¹ and the approximate location of the array and the wayside cabinet are indicated in **Figure 1**.

Figure 1 Approximate location of the pavement array (red) and wayside cabinet (yellow)



The array consists of nine sensors embedded in seven holes which are named alphabetically A to G. Photos of the sensor array are shown in **Figure 2**. The array's centreline (holes C, F and G) is nominally 700 mm from the centre of the edge line (**Figure 3**). **Figure 3** identifies principal dimensions of the array.



¹ Estimated from google.com.au/maps and to be confirmed during TSD trials.

Figure 2 Sensor array

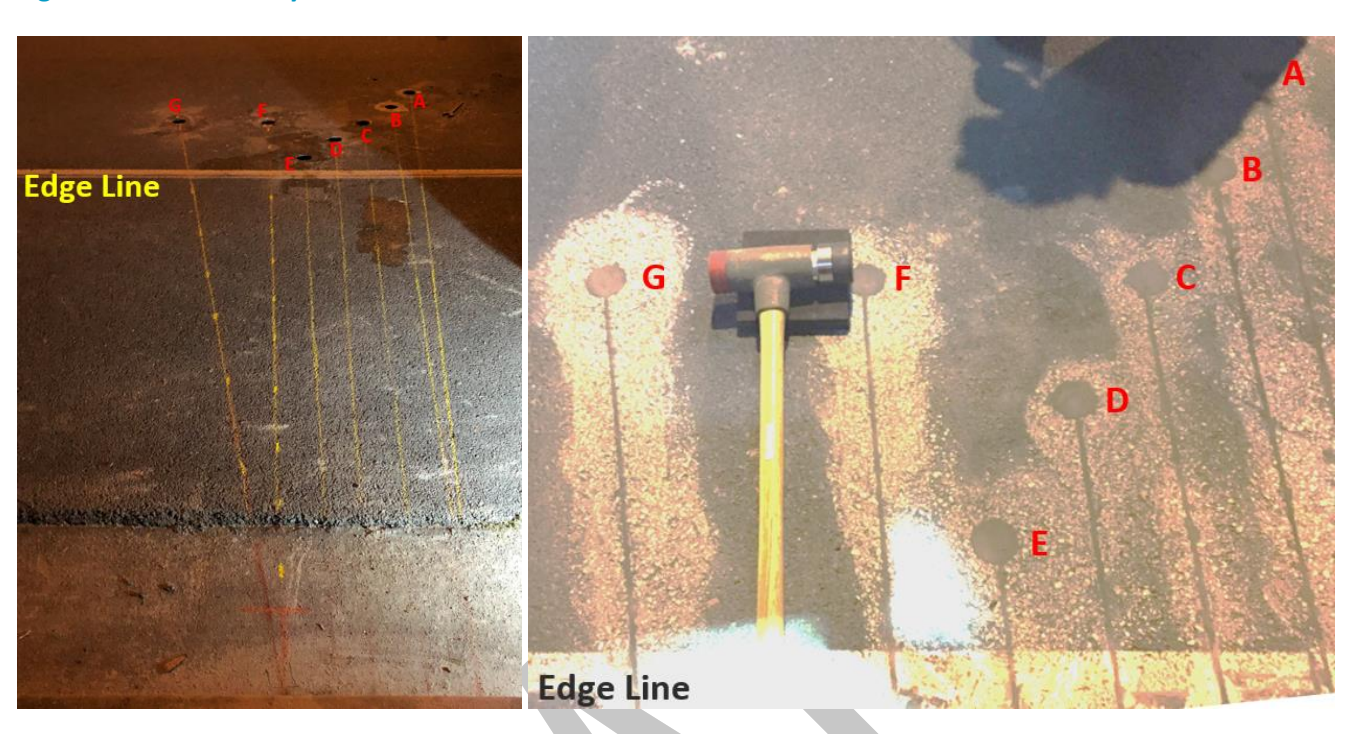


Figure 3 Array geometry and sensor type

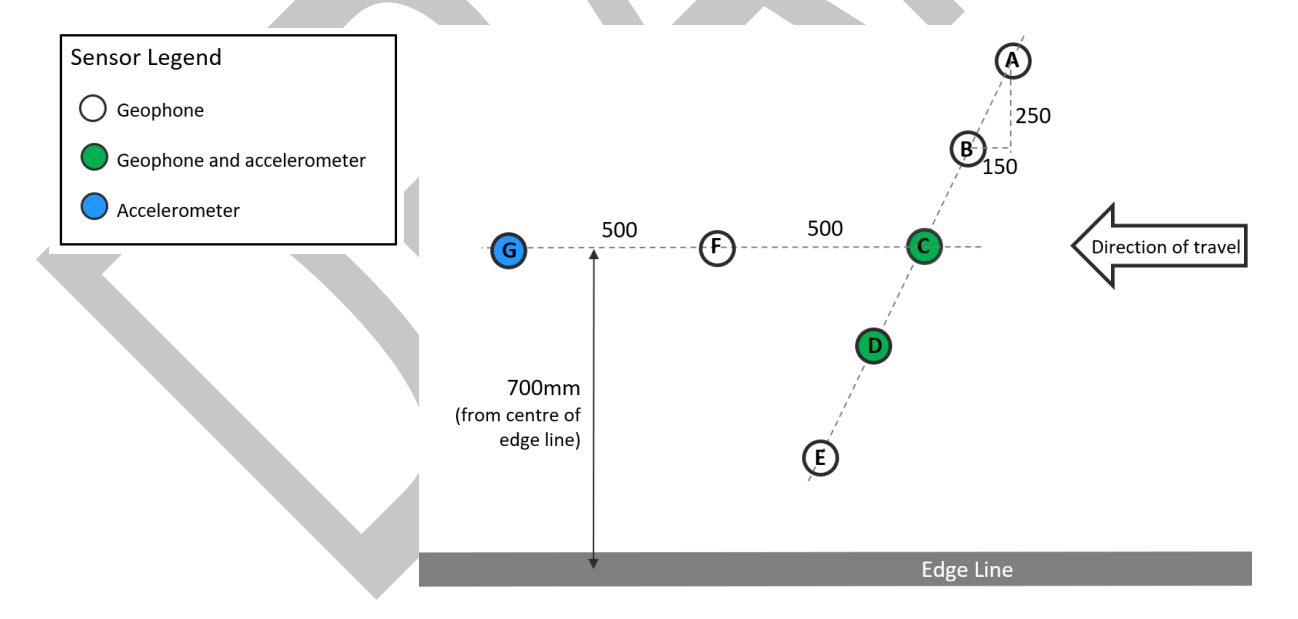


Table 1 shows detailed photographs of each hole before the resin was poured. **Appendix A** contains a general description of the sensor encapsulation and **Appendix B** contains the geophone calibration sheets and lists the accelerometers sensitivities. The following sensors were used:

• Geophone (holes A, B, C, D, E, F): Model HG6-UB manufactured by HGS (India) Limited.



- Accelerometers (holes C, D): Model 3305A3 manufactured by Dytran.
- Accelerometer (hole G): Model 728T manufactured by Wilcoxon.

The sensors for each hole were prepared in SLR's Sydney office. From past experience gained on similar projects, the sensor enclosure design ensured that the sensor itself is shielded from the vertical loads created by traffic. All sensor enclosures had a M6 anchor bolts fitted to their bases. The anchors were epoxy glued into pilot holes which were drilled into the bases of the coreholes. All holes were cored with a diameter 72 mm drill bit and the depth of the core holes ranged from 70 mm to 90 mm, depending on the type(s) of sensor(s) installed. The core holes were filled with resin, completely immersing the enclosures. The resulting resin covers from the top of the sensor enclosure to the pavement surface ranged from 10 mm to 23 mm.

Table 1 Instrumentation

Hole	Photo	Comments
A		Geophone S/N 583-V3 Resin cover: approximately 16 mm
В	829	Geophone S/N 829-V3 Resin cover: approximately 23 mm
С	581	Geophone S/N 581-V3 Accelerometer S/N 10643 Resin cover: approximately 20 mm



Hole	Photo	Comments
D		Geophone S/N 827-V3 Accelerometer S/N 10646 Resin cover: approximately 14 mm
Е	826	Geophone S/N 826-V3 Resin cover: approximately 10 mm from top of foam cap.
F	830	Geophone S/N 830-V3 Resin cover: approximately 15 mm
G		Accelerometer S/N 5378 Resin cover: approximately 17 mm from top of foam cap.



Deception Bay Road, Deception Bay, QLD

3 Conclusions

This report presents the sensors, sensor enclosures and sensor layout installed at the permanent pavement installation site on Deception Bay Road in Deception Bay, Queensland.





APPENDIX A

Sensor Encapsulation



Single Geophones (hole A, B, E, F)

HG6-UB geophones with nominal sensitivities of 28.8 mm/s were used. The geophones are nominally 4.5 Hz resonant.

The schematic sensor build up for geophones only sensors is shown in **Figure 4**. Additional photos during different stages of the installation are shown in **Figure 5**.

The PVC endcap at the top was shortened to minimise the sensor height. The two PVC caps were taped together. A two core lead was soldered to the geophone terminals and hotglued to the top of the geophone. In addition, the lead was strain relieved with tape (**Figure 5**).

Figure 4 Geophone only encapsulation schematic

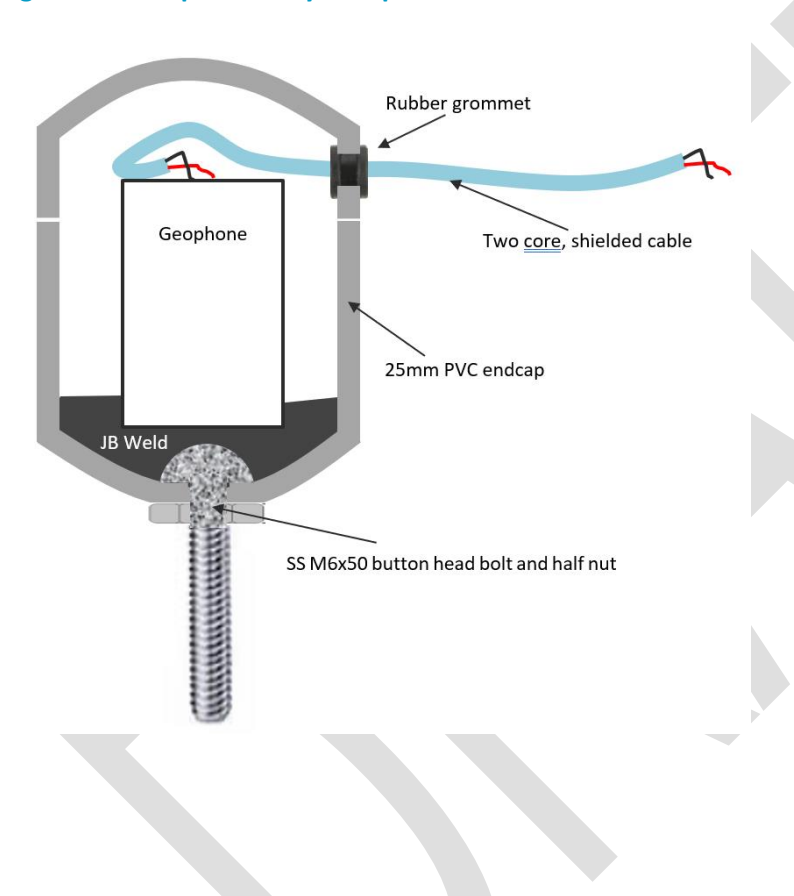


Figure 5 Geophone only sensor preparation photos



Geophone and Accelerometer (hole C, D)

HG6-UB geophones with nominal sensitivities of 28.8 mm/s were used. The geophones are nominally 4.5 Hz resonant. Dytran model 330A03 IEPE accelerometers with nominal sensitivities of 500 mV/g were used. A schematic sensor build up is shown in **Figure 6**.

The two PVC caps holding the accelerometer and geophone are held together via the anchor bolt. In addition, the gap between the two caps has been filled with JB weld. The PVC cap at the top was cut short to minimise the overall height and taped to the center PVC cap holding the geophone. A two core lead was soldered to the geophone terminals and hotglued to the top of the geophone. In addition, the lead was strain relieved with tape. The microdot lead from the accelerometer was guided to the rubber grommet at the top and protected by a vinyl tubing.

Figure 6 Combined geophone and accelerometer encapsulation schematic

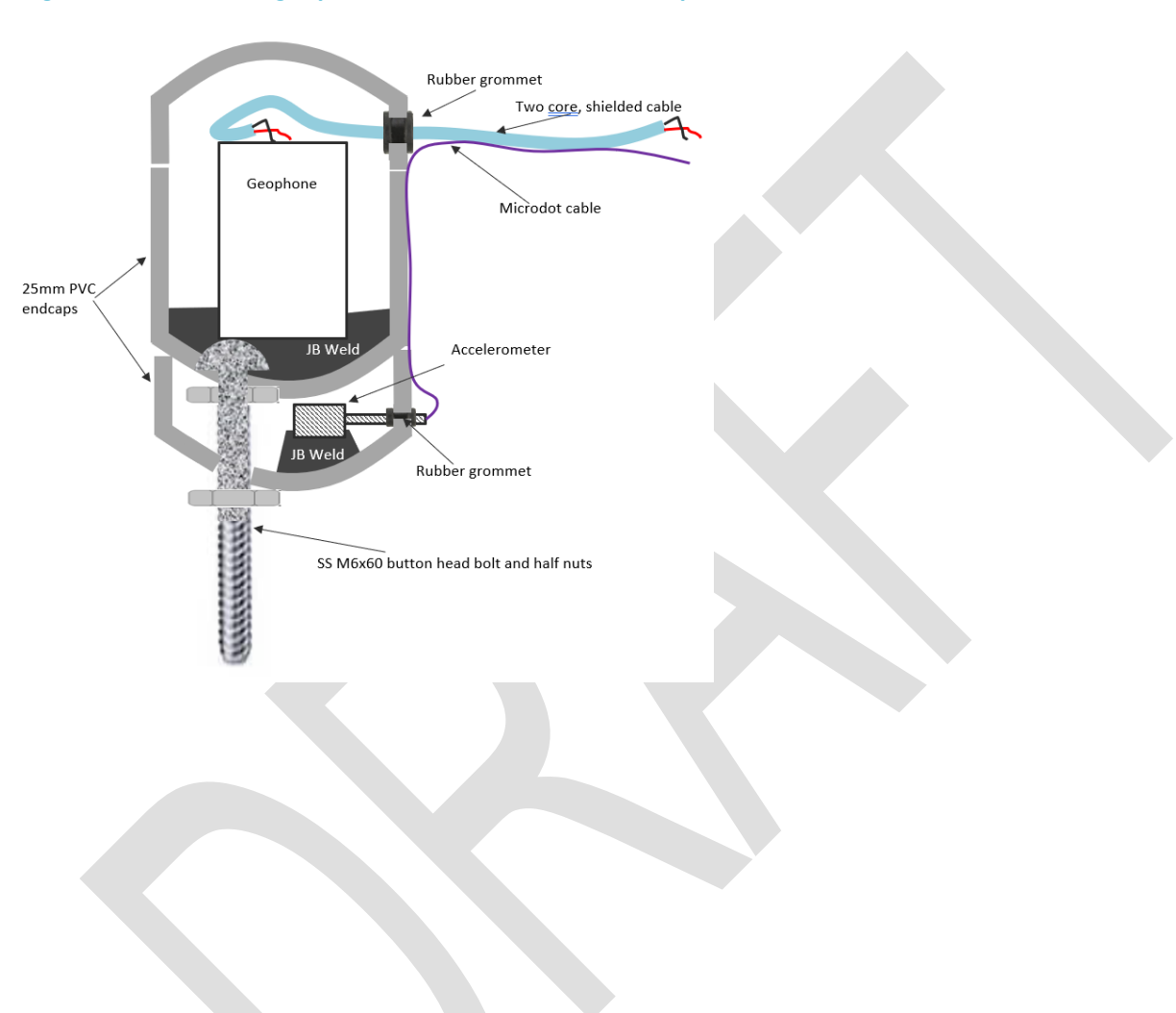
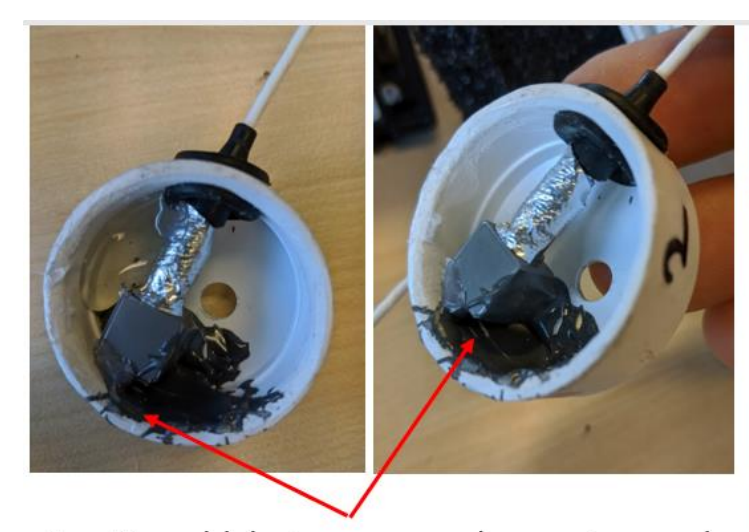


Figure 7 Combined geophone and accelerometer preparation photos



No JB weld between accelerometer and the side of the cap.





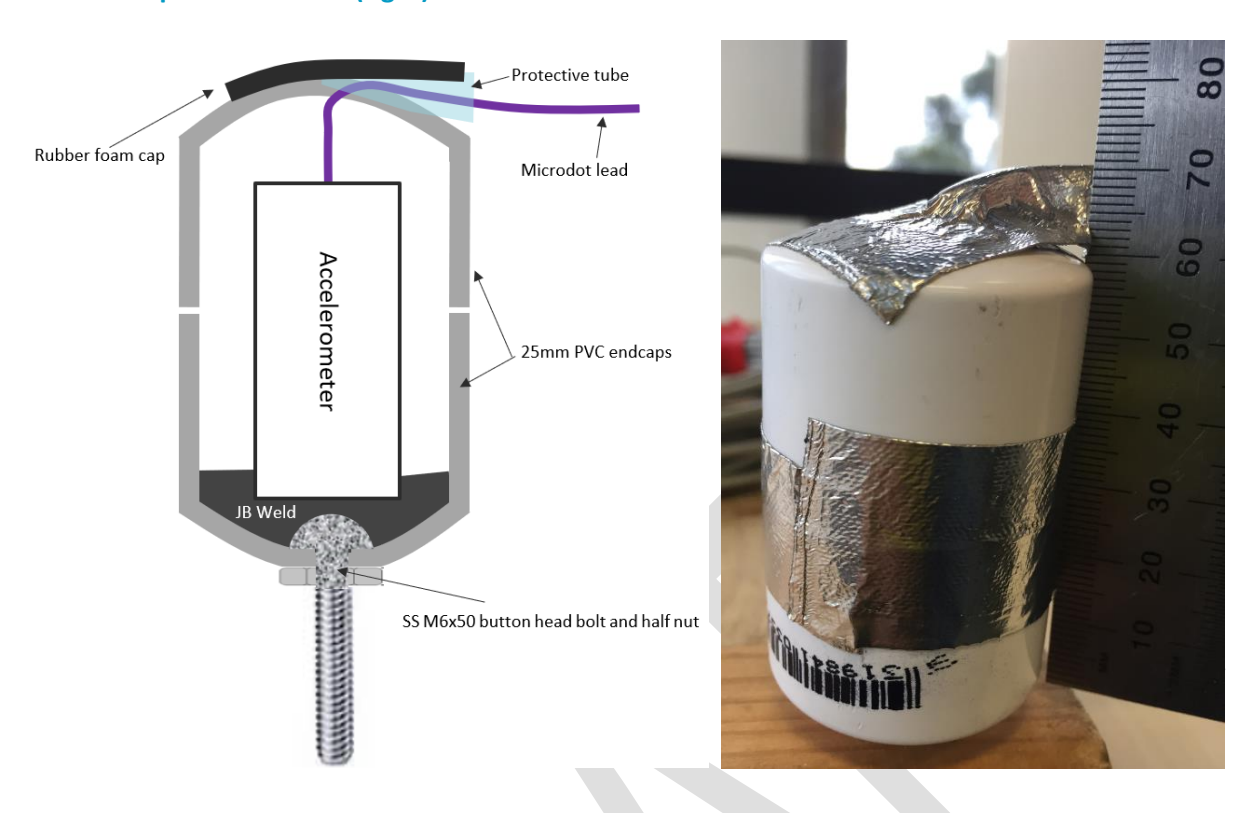
Protective tubing.

Single Accelerometer (hole G)

A Wilcoxon model 728T IEPE accelerometer with a nominal sensitivity of 500 mV/g was used.

The schematic sensor build up and a photo are shown in **Figure 8**. The two PVC caps were taped together and the exit hole at the top was sealed with tape.

Figure 8 Accelerometer only encapsulation schematic (left) and closed capsule without the rubber cap and protective tube (right).





APPENDIX B

Sensor Sensitivities



Page 15

Sensor Type: HG6-UB
Assembly Version: 2019-18
Serial Number: 581-V3

Description: Velocity Transducer Final Acceptance Data Method: Back-to-Back Comparison Calibration

Calibration Data

 Sensitivity @ 80 Hz:
 29.62
 V/m/s

 Damping:
 0.560

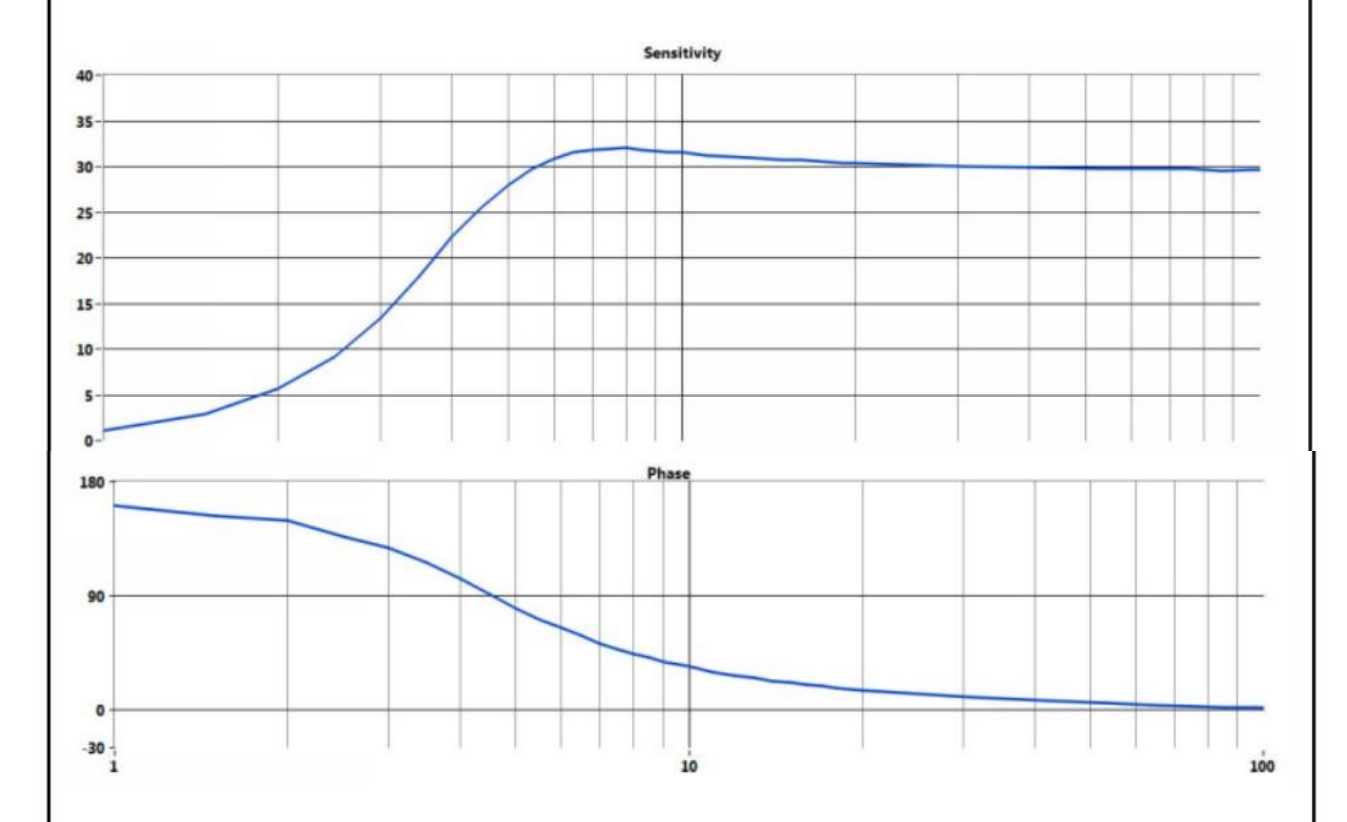
 Frequency:
 4.64
 Hz



HGS (INDIA) LIMITED 158, Sector-4 IMT Manesar

158, Sector-4 IMT Manesar Gurgaon, Haryana-122050-India Phone: +91 124 4681800

Fax: +91 124 4681845 www.hgsindia.com



Data Points

Temper	ature:	20 C				Relative Humidity:		42 %
Frequer	ncy (Hz)							
1	2	5	10	20	40	60	80	100
Sensitiv	rity (V/m/s)							
1.1	5.7	28.0	31.6	30.4	29.9	29.8	29.6	29.6

Notes

1. This certificate shall not be reproduced, except in full, without written approval from HGS India Limited

2. See Manufacturer's Specification Sheet for a detailed listing of performance specifications

Date: 2018.07.09 Page 1/1



Sensor Type: HG6-UB
Assembly Version: 2019-18
Serial Number: 583-V3

Description: Velocity Transducer Final Acceptance Data
Method: Back-to-Back Comparison Calibration

Calibration Data

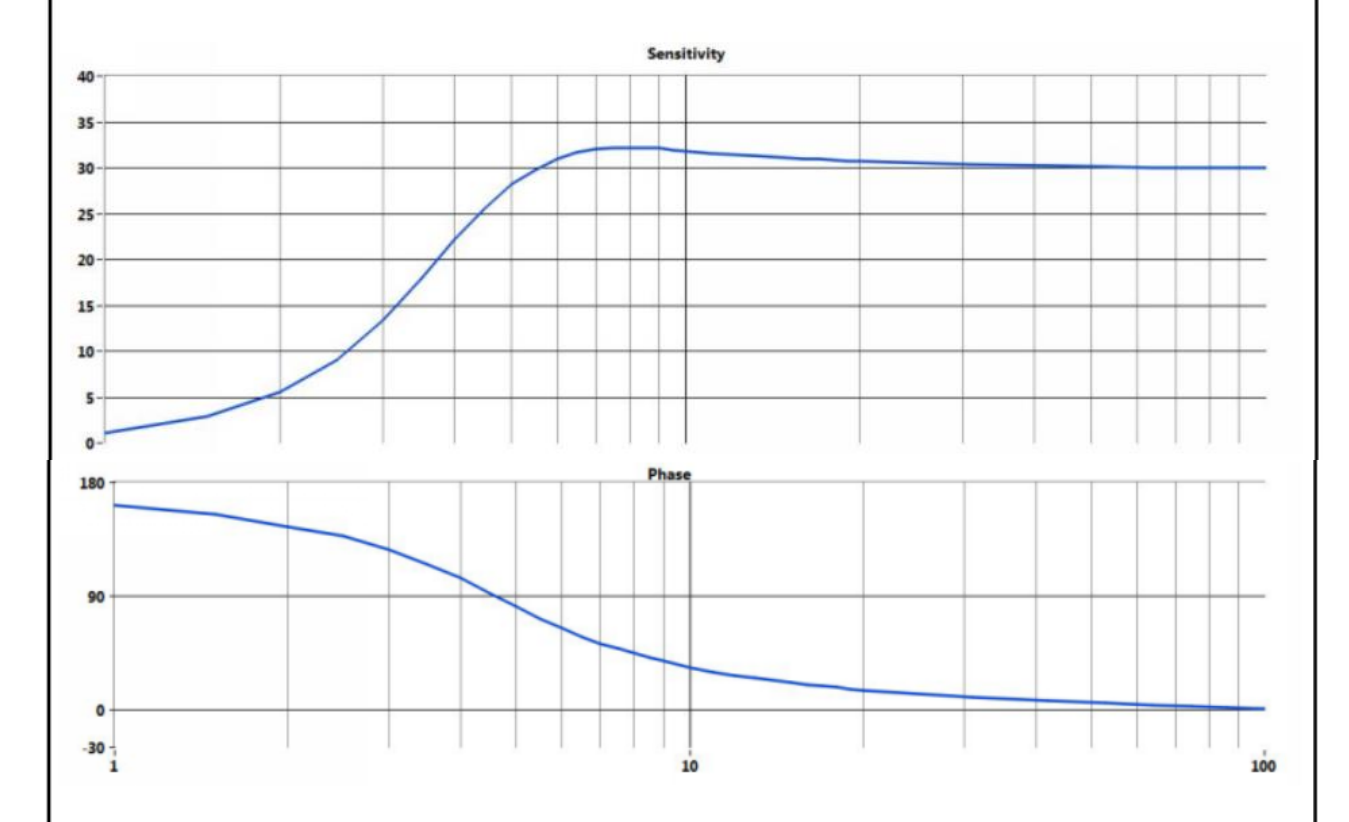
Sensitivity @ 80 Hz: 30.00 V/m/s Damping: 0.565 -Frequency: 4.67 Hz



HGS (INDIA) LIMITED

158, Sector-4 IMT Manesar Gurgaon, Haryana-122050-India Phone: +91 124 4681800

Fax: +91 124 4681845 www.hgsindia.com



Data Points

Temper	rature:	20 C				Relative	Humidity:	42 %
Frequer	ncy (Hz)							
1	2	5	10	20	40	60	80	100
Sensitiv	ity (V/m/s)							
1.1	5.5	28.2	31.8	30.7	30.2	30.1	30.0	30.0

Notes

1. This certificate shall not be reproduced, except in full, without written approval from HGS India Limited

See Manufacturer's Specification Sheet for a detailed listing of performance specifications

Date: 2018.07.31 Page 1/1



Sensor Type: HG6-UB
Assembly Version: 2020-19
Serial Number: 826-V3

Description: Velocity Transducer Final Acceptance Data Method: Back-to-Back Comparison Calibration

Calibration Data

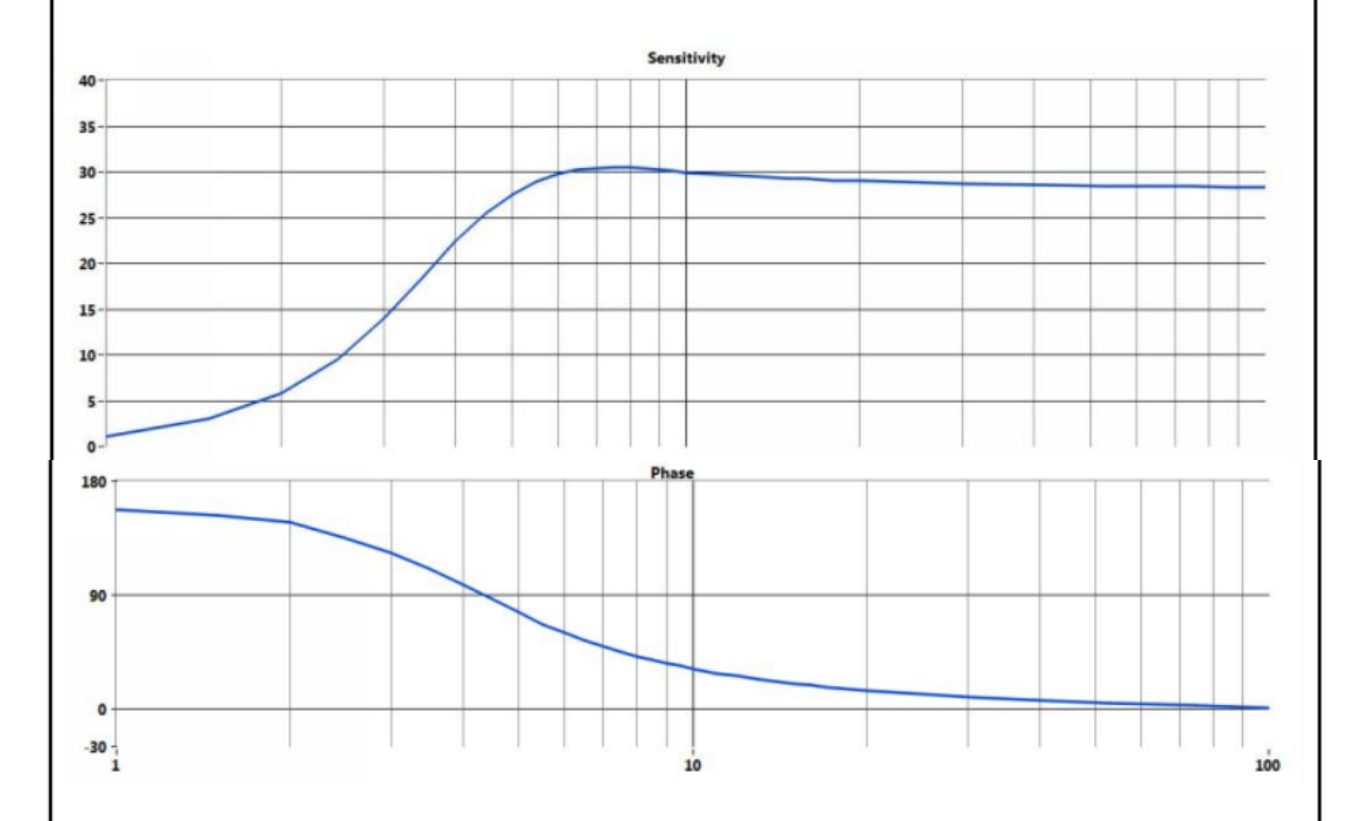
Sensitivity @ 80 Hz: 28.35 V/m/s Damping: 0.564 -Frequency: 4.45 Hz



HGS (INDIA) LIMITED

158, Sector-4 IMT Manesar Gurgaon, Haryana-122050-India Phone: +91 124 4681800

Fax: +91 124 4681845 www.hgsindia.com



Data Points

Tempe	rature:	20 C				Relative	42 %	
Freque	ncy (Hz)							
1	2	5	10	20	40	60	80	100
Sensitiv	vity (V/m/s)							
1.1	5.7	27.5	29.9	29.0	28.6	28.4	28.3	28.3

Notes

1. This certificate shall not be reproduced, except in full, without written approval from HGS India Limited

2. See Manufacturer's Specification Sheet for a detailed listing of performance specifications

Date: 2019.02.12 Page 1/1



Sensor Type: HG6-UB
Assembly Version: 2020-19
Serial Number: 827-V3

Description: Velocity Transducer Final Acceptance Data
Method: Back-to-Back Comparison Calibration

Calibration Data

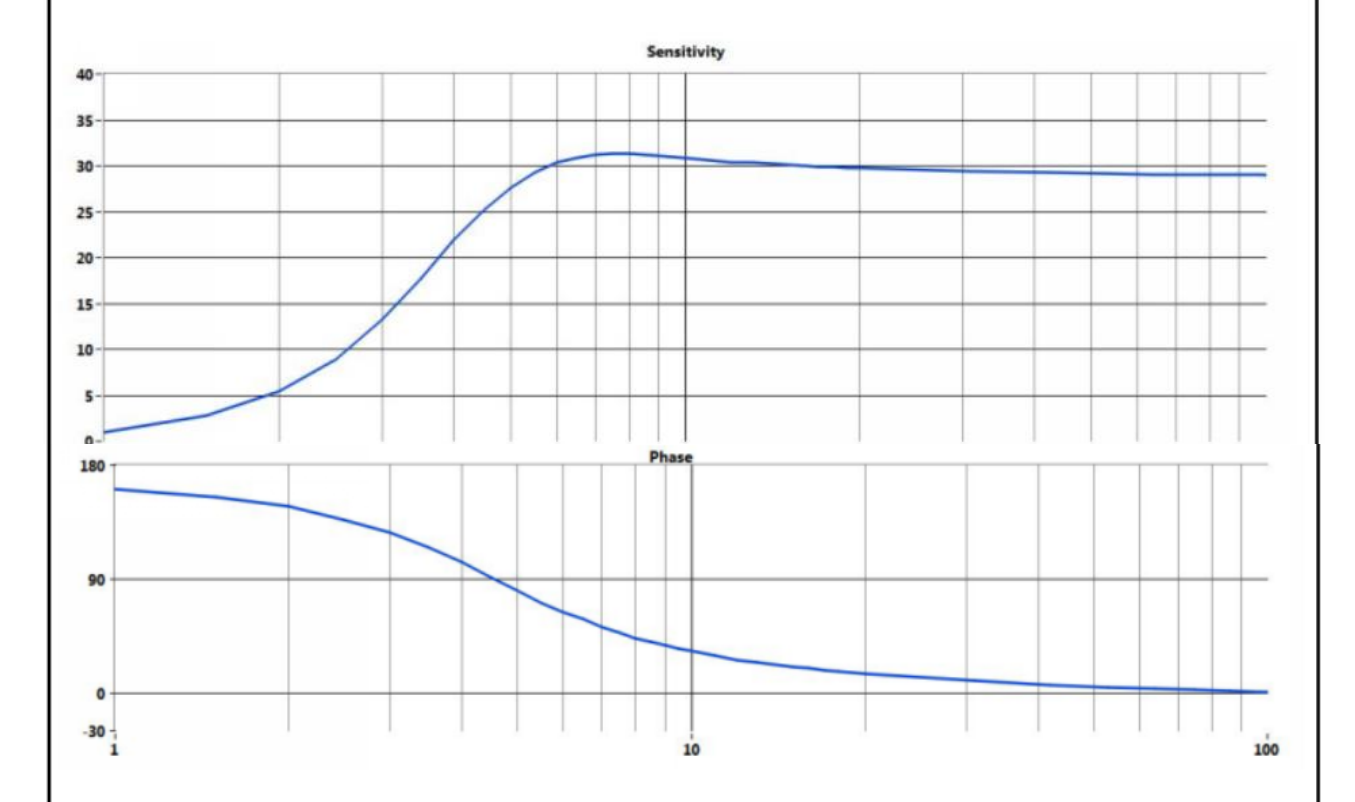
Sensitivity @ 80 Hz: 29.02 V/m/s
Damping: 0.559 Frequency: 4.64 Hz



HGS (INDIA) LIMITED

158, Sector-4 IMT Manesar Gurgaon, Haryana-122050-India

Phone: +91 124 4681800 Fax: +91 124 4681845 www.hgsindia.com



Data Points

_									
Т	emperature	: :	20 C				Relative Hun	nidity:	42 %
F	requency (F	Hz)							
1	l.	2	5	10	20	40	60	80	100
S	Sensitivity (\	V/m/s)							
1	.0	5.5	27.6	30.9	29.8	29.3	29.1	29.0	29.0

Notes

1. This certificate shall not be reproduced, except in full, without written approval from HGS India Limited

2. See Manufacturer's Specification Sheet for a detailed listing of performance specifications

Date: 2019.02.12 Page 1/1



HG6-UB Sensor Type: 2020-19 Assembly Version: 829-V3 Serial Number:

Description: Velocity Transducer Final Acceptance Data Method: Back-to-Back Comparison Calibration

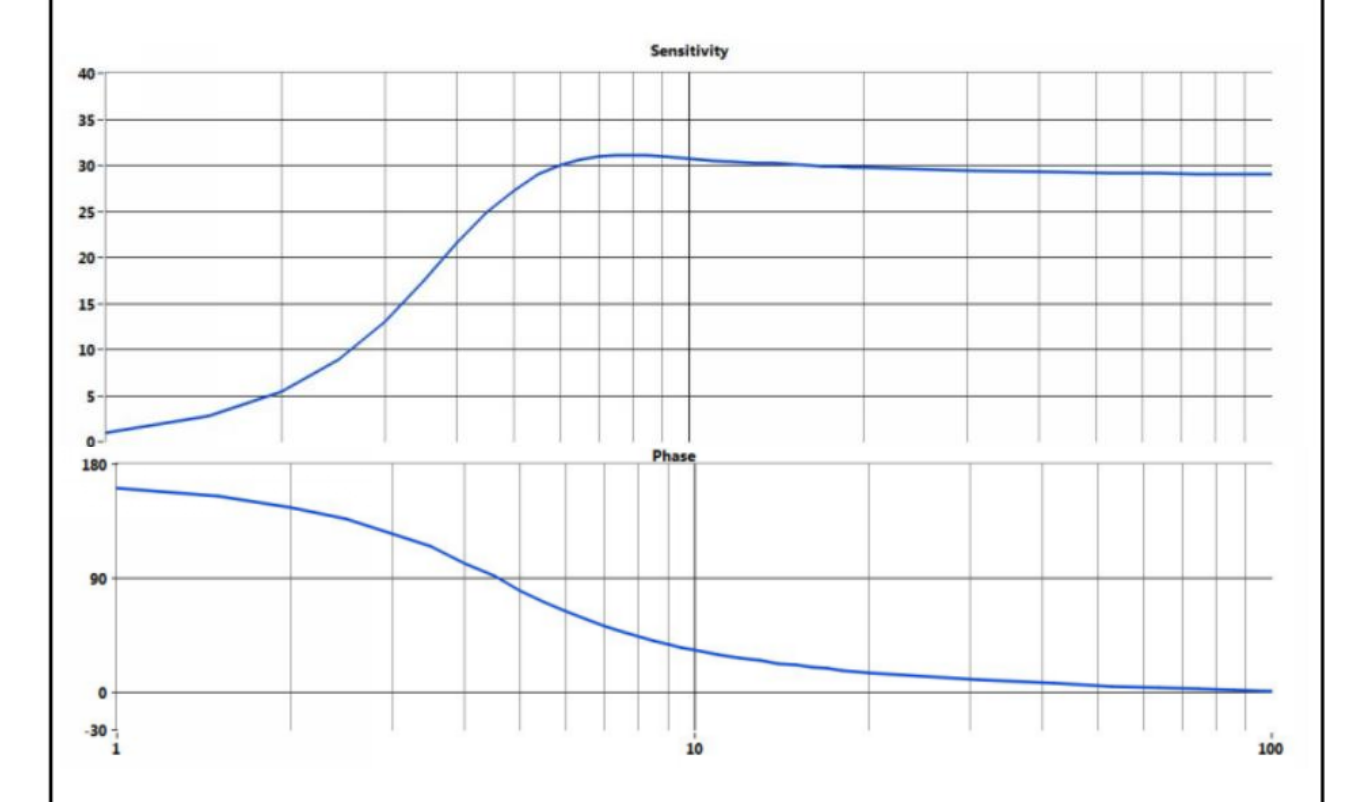
Calibration Data

Sensitivity @ 80 Hz: 29.06 V/m/s Damping: 0.566 Frequency: 4.64 Hz



HGS (INDIA) LIMITED 158, Sector-4 IMT Manesar Gurgaon, Haryana-122050-India

Phone: +91 124 4681800 +91 124 4681845 www.hgsindia.com



Data Points

_									
Temperature:			20 C			Relative Humidity:		42 %	
F	requency (Hz)							
1		2	5	10	20	40	60	80	100
5	Sensitivity (V/m/s)							
1	.0	5.4	27.3	30.7	29.8	29.3	29.1	29.1	29.0

Notes

This certificate shall not be reproduced, except in full, without written approval from HGS India Limited

2. See Manufacturer's Specification Sheet for a detailed listing of performance specifications

Date: 2019.02.12 Page 1/1



Sensor Type: HG6-UB
Assembly Version: 2020-19
Serial Number: 830-V3

Description: Velocity Transducer Final Acceptance Data
Method: Back-to-Back Comparison Calibration

Calibration Data

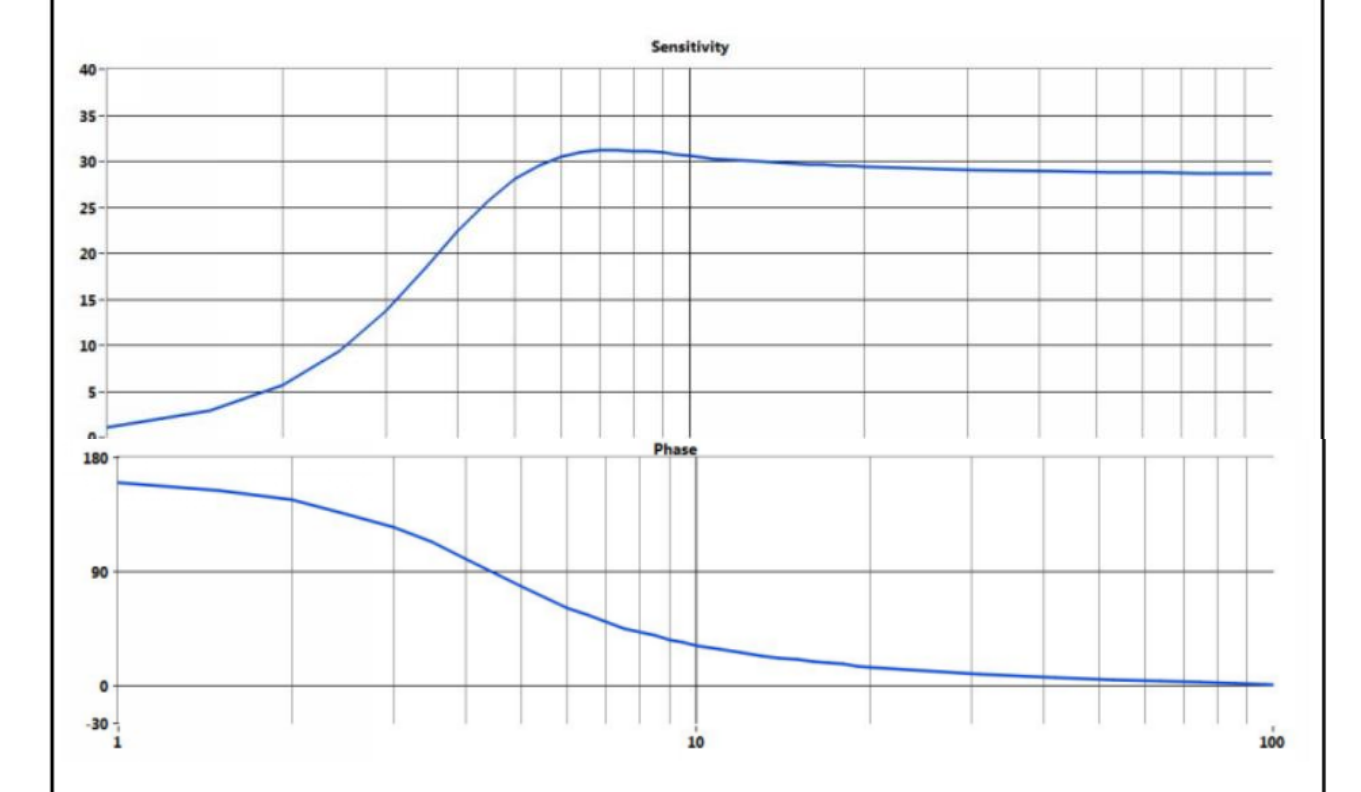
Sensitivity @ 80 Hz: 28.69 V/m/s Damping: 0.552 -Frequency: 4.55 Hz



HGS (INDIA) LIMITED

158, Sector-4 IMT Manesar Gurgaon, Haryana-122050-India

Phone: +91 124 4681800 Fax: +91 124 4681845 www.hgsindia.com



Data Points

Tempe	rature:	20 C				Relative	42 %	
Freque	ncy (Hz)							
1	2	5	10	20	40	60	80	100
Sensitiv	vity (V/m/s)							
1.1	5.6	28.0	30.6	29.4	28.9	28.8	28.7	28.6

Notes

1. This certificate shall not be reproduced, except in full, without written approval from HGS India Limited

2. See Manufacturer's Specification Sheet for a detailed listing of performance specifications

Date: 2019.02.12 Page 1/1

The sensitivities of the accelerometers are:

1) Dytran S/N 10643: 495.96 mV/g

2) Dytran S/N 10646: 499.35 mV/g

3) Wilcoxon S/N 5378: 503 mV/g





Calibration Data

General Purpose Accelerometer

	Model 728T	Serial Number 5378
Sensitivity:	503 mV/g	51.3 mV/m/s ²
Bias Voltage:	9.8 Vdc	
Resonance:	20.0 kHz	1198.08 kcpm
Maximum Amplitude Range:	15 g peak	147 m/s² pk
Transverse Sensitivity:	1 %	
Frequency Response:		
±5%:	2.0 Hz to 5.8 kHz	120 cpm to 348 kcpm
±10%:	1.2 Hz to 10.7 kHz	72 cpm to 640 kcpm
±3dB:	0.8 Hz to kHz	48 cpm to

Calibrated by: T.PHOUBANDITH

This calibration is traceable to the National Institute of Standards and Technology, Gaithersburg, MD 20899.

Frequency Response is traceable 5 Hz to 10 kHz.

Sensitivity measured at 100 Hz, 1g, 25°C.

Low end frequency response and amplitude range are nominal values.

Wilcoxon Sensing Technologies is an ISO 9001 Registered Company.

Date: 07/12/2019

ASIA PACIFIC OFFICES

BRISBANE

Level 2, 15 Astor Terrace Spring Hill QLD 4000 Australia

T: +61 7 3858 4800 F: +61 7 3858 4801

MACKAY

21 River Street Mackay QLD 4740 Australia

T: +61 7 3181 3300

SYDNEY

2 Lincoln Street Lane Cove NSW 2066 Australia

T: +61 2 9427 8100 F: +61 2 9427 8200

AUCKLAND 68 Beach Road

Auckland 1010 New Zealand T: +64 27 441 7849

CANBERRA

Australia

GPO 410 Canberra ACT 2600

T: +61 2 6287 0800 F: +61 2 9427 8200

MELBOURNE

Suite 2, 2 Domville Avenue Hawthorn VIC 3122 Australia

T: +61 3 9249 9400 F: +61 3 9249 9499

TOWNSVILLE

Level 1, 514 Sturt Street Townsville QLD 4810 Australia

T: +61 7 4722 8000 F: +61 7 4722 8001

NELSON

6/A Cambridge Street Richmond, Nelson 7020

New Zealand T: +64 274 898 628

DARWIN

Unit 5, 21 Parap Road Parap NT 0820 Australia

T: +61 8 8998 0100 F: +61 8 9370 0101

NEWCASTLE

10 Kings Road
New Lambton NSW 2305
Australia
T: +61.24037 3200

T: +61 2 4037 3200 F: +61 2 4037 3201

TOWNSVILLE SOUTH

12 Cannan Street Townsville South QLD 4810 Australia

T: +61 7 4772 6500

GOLD COAST

Level 2, 194 Varsity Parade Varsity Lakes QLD 4227 Australia

M: +61 438 763 516

PERTH

Ground Floor, 503 Murray Street
Perth WA 6000
Australia

T: +61 8 9422 5900 F: +61 8 9422 5901

WOLLONGONG

Level 1, The Central Building UoW Innovation Campus North Wollongong NSW 2500 Australia

T: +61 404 939 922

APPENDIX B TMR DRAFT TECHNICAL NOTE

Technical Note 182

Deflection Testing of Roads with Traffic Speed Devices

April 2019



Feedback: Please send your feedback regarding this document to: tmr.techdocs@tmr.qld.gov.au

i

1 Introduction

The aim of the Technical Note is to provide information and guidance on use of Traffic Speed Deflectometer (TSD) technology in pavement condition assessment. The potential for TSD to be used in pavement rehabilitation design is explored.

The main feature of the technical note is to present a practical procedure to back-calculate pavement layer moduli from TSD data. This can be performed by first converting the TSD deflection velocity slope measurements to near equivalent FWD deflection. The back-calculation software developed for the FWD device could then be employed to back-calculate TSD measurements. This approach facilitates the use of TSD data with the already established FWD back-calculation procedure.

The procedures outlined in technical note are considered interim and are likely to be updated in the future when more experience has been gained from the application.

2 Background

The TSD attempts to measure the vertical velocities of the pavement surface deflections while travelling at traffic speed (nominally 80 km/h). By interpolating the velocities measured by a series of Doppler lasers located at discrete longitudinal offsets from the centre of load and then integrating the results over time it is possible obtain a deflection bowl which can be compared with that produced by other devices including the Falling Weight Deflectometer (FWD), Deflectograph and Benkelman Beam.

A study carried out by (Baltzer et al, 2010) on 18,000 km road network in New South Wales and Queensland concluded that the three measuring devices (Deflectograph, FWD and TSD) showed virtually identical profiles of bearing capacity. The TSD results provide good agreement for characterising the strength of the pavements compared with the conventional methods. An evaluation of the TSD measurements conducted by Austroads (Robert et al, 2014) demonstrated that correlation (R² varies from 0.71 to 0.90) exists between the maximum deflection measures of the FWD and TSD and the correlation confirmed the ability of the TSD to differentiate between weak and strong structures for typical Australian and New Zealand flexible pavements. The Austroads study showed that for the Queensland sites, it was possible to derive consistent and AUTC-based outcomes for a very wide range of deflection values, location and climates.

The TSD was developed by Greenwood Engineering A/S (https://www.greenwood.dk/index.php) during the early 2000s and was first trialled in Australia in 2009/2010 (Kelly & Moffatt, 2012).

With the support of several state road agencies the ARRB Group acquired a TSD in 2014 to carry out network level surveys in New South Wales, Queensland and New Zealand (Roberts et al, 2014).

Testing in Queensland is generally carried out during the four month period between April and August each year. During this period, it is possible to measure approximately half the state road network.

While in Queensland the TSD spends most of its time collecting network level data as described in the department's Data Collection Policy.

Although the TSD technology is intended to collect the slope velocities of the deflected pavement surface, it is deployed on a vehicular platform referred to as the Intelligent Pavement Assessment Vehicle (iPave) which collects a variety of additional information. These include: chainage, global navigation satellite system (GNSS) coordinates, roughness, rut depth, texture depth, horizontal curvature, vertical curvature, gradient, crossfall and video.

3 Key Differences

There are different deflection testing devices available on the market and FWD has been the 'standard' in deflection testing for over the past four decades. Table 1 summarises the characteristics of them. There are two key differences when comparing the TSD with the FWD, namely: Firstly, FWD applies an impact load while a TSD is a moving wheel load; Secondly, FWD uses geophones to measure the pavement surface deflection while a TSD uses Doppler lasers to measure the slope velocities of the pavement surface deflection.

	Benkelman Beam	Deflectograph	Falling Weight Deflectometer	Traffic Speed Deflectometer
Speed of waveform while measuring	Stationary	1 m/s (3.5 km/h vehicle speed)	180 to 600 m/s (speed of Rayleigh waves)	180 to 600 m/s +/- 22 m/s (80 km/h vehicle speed)
Data generated by the device	Deflection	Deflection	Deflection	Slope velocities of deflected pavements

4 Models for Converting TSD Data

The TSD attempts to measure the vertical velocity of the pavement surface while travelling at traffic speed (nominally 80 km/h). By interpolating the velocity measured by a series of Doppler lasers located at discrete longitudinal offsets from the centre of load, to obtain the deflection bowl. Then, parameters such as the maximum deflection, curvature and other structural condition indices can be derived from the deflection bowl. Two methods are available to convert TSD deflection slope to deflection are as follows:

- Euler-Bernoulli beam model (Rasmussen et al, 2008) or commonly known as "Greenwood Model".
- ARRB "area under the curve" (AUTC) method (Roberts & Byrne, 2008) and (Muller & Roberts, 2013)

During operations, Doppler sensors measure vertical velocities of the deflected pavement surface at the discrete points and when divided by the instantaneous vehicle speed, they produce deflection slopes (V_v/V_h) at those points (Rasmussen et al, 2008). Figure 1 shows the pavement deflection velocity vectors under a rolling wheel. Together with the deflection velocity the corresponding deflection basin is shown in Figure 2 where deflection slopes (tangents) are displayed. To determine the actual pavement deflections, deflection slope curve must be integrated using a closed-form solution of a mechanical model such as an elastic beam on Winkler foundation (Rasmussen et al, 2008). This is expressed in the Euler-Bernoulli beam as shown in equation 1:

$$EI\frac{d^4}{dx^4}w(x) + kw(x) = -F(x)$$

(1)

where, F is the point force, E the elasticity, I the moment of inertia, h the pavement thickness and k is the spring constant.

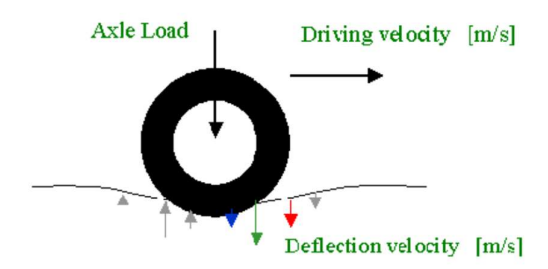


Figure 1. Pavement deflection velocity under a rolling load (Rasmussen et al., 2008).

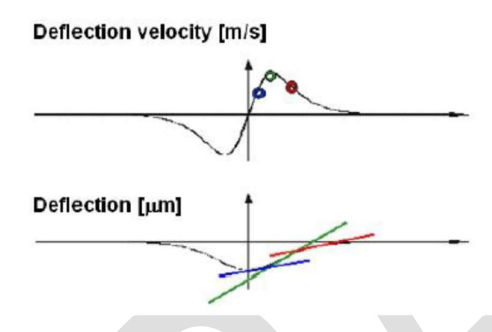


Figure 2. Pavement deflection velocity and deflection basin with deflection slopes (tangents) (Rasmussen et al., 2008).

The current algorithm being used by the manufacturer is built on a statistical method that fits a curve through TSD measured data (Padersen, 2013) and it also accounts for asymmetry in deflection basin (Nasimifar, 2017).

The AUTC method was developed following the initial TSD trials in Australia in 2010 (Roberts et al, 2014). The AUTC model involves fitting the TSD slope measurements and numerically integrating over the length of the deflection bowl, working towards the wheel load in accordance with the following procedures:

- The base TSD data consists of a set of vertical pavement velocities, referenced against
 horizontal offset spaced along the axis of the wheel path and away from the loading of the
 dual tyred truck wheels. This data is termed the velocity profile.
- The value of the velocity at each point is a function of the pavement strength, the offset of the
 Doppler laser, velocity sensor from the centre point of loading, and the horizontal speed of the
 TSD vehicle (which affects the speed of the vertical loading).
- The slope is the ratio between the vertical and horizontal velocities at each measurement point and actual physical slope of the pavement surface within the deflection bowl centred under the moving TSD vehicle rear wheel.

- By plotting slope values against offsets from the load point as a slope profile curve (analogous
 to the previously mentioned velocity profile), it is possible to show that the cumulative area
 under the slope profile working from the tail is exactly equal to the vertical deflection at that
 point.
- The vertical difference between any two deflection points, such as for the bowl curvature, (D₀-D₂₀₀), is equal to the area under the slope profile curve between these two points.

Full text of the AUTC procedures can be found in Austroads Publication No. AP-T279-14 (Roberts et al., 2014).

5 Test Models

Austroads prepared two publications on the test method and specification on the use of the TSD device, which is listed in Table 2.

Table 2. List of Austroads Test Methods on TSD

Austroads Test Method	Title
AG:AM/T017 (Austroads, 2016a)	Pavement data collection with a Traffic Speed Deflectometer (TSD) device
AG:AM/S006 (Austroads, 2016b)	Specification for pavement deflection measurement with a Traffic Speed Deflectometer (TSD) device

6 TSD Output Parameters and Data Validity

Raw data from the Doppler Lasers collected by the TSD are processed by the Greenwood Engineering software "Profilograph for Windows". The output has a minimum reporting interval of 10m. To convert the TSD slope measurement to deflection values, two models as mentioned in Section 4, namely, (i) Greenwood's Asymmetric model. (Murnane et al., 2017) and (ii) ARRB Area Under the Curve (AUTC) model (Roberts & Byrne, 2008) and (Muller & Roberts, 2013)

The Greenwood model only supplies a bowl deflection in six locations 0 to 900 mm from the load, with the algorithm using the optimised Euler-Bernoulli Beam model. The AUTC model supplies a full nine points bowl from 0 to 1500 mm from the load). This model is not an explicit model as the one from Greenwood. The AUTC model involves fitting the TSD slope measurements and numerically integrating over the length of the deflection bowl, working towards the wheel load. This provides a simple approach in converting the slope profile to vertical deflections at that point as compared to the Greenwood model.

The TSD deflection reported for TMR was processed using the AUTC model. The AUTC model supplies a full nine points bowl from 0 to 1500 mm from the load.

The collected survey data from TSD is reported in the format detailed in Austroads Technical Note AG:AM/S006. The information other than the location of the survey that is relevant to pavement engineer are listed as follows:

Table 3 List of output parameters reported by the TSD

Table 3 List of output parameters reported by the TSD

Database field description	Field name
Mean vehicle speed for interval (km/h)	SPEED
Surface temperature from infra-red thermometer (°C)	SURF_TEMP
Outside air temperature (°C)	AIR_TEMP
Strain Gauge Left Axle Load (kg)	S_GAUGE_LEFT
Strain Gauge Right Axle Load (kg)	S_GAUGE_RIGHT
Slope 0.10 – Gradient slope measurement at 100 mm from load (μm/m)	SLP100
Slope 0.20 – Gradient slope measurement at 100 mm from load (μm/m)	SLP200
Slope 0.30 – Gradient slope measurement at 100 mm from load (μm/m)	SLP300
Slope 0.45 – Gradient slope measurement at 100 mm from load (μm/m)	SLP450
Slope 0.60 – Gradient slope measurement at 100 mm from load (μm/m)	SLP600
Slope 0.90 – Gradient slope measurement at 100 mm from load (μm/m)	SLP900
Curvature (μm)	CURV
SCI SUB – Structural Condition Index Subgrade (μm)	SCI_SUBGRADE
Deflection 0 – Deflection calculation at 0 mm from load (μm)	TD0
Deflection 200 – Deflection calculation at 0 mm from load (μm)	TD200
Deflection 300 – Deflection calculation at 0 mm from load (μm)	TD300
Deflection 450 – Deflection calculation at 0 mm from load (μm)	TD450
Deflection 600 – Deflection calculation at 0 mm from load (μm)	TD600
Deflection 900 – Deflection calculation at 0 mm from load (μm)	TD900
Deflection 1200 – Deflection calculation at 0 mm from load (μm)	TD1200
Deflection 1500 – Deflection calculation at 0 mm from load (μm)	TD1500
Event code (Note 1)	ECODE

Note 1: Event code reports discrete events such as bridge abutment and railway crossing. It also indicates the reason for any invalid data. For more details refer to AG:AM/S006.

The following is a list event codes indicating invalid data:

- **W** (Road works)
- **S** (Speed or distance outside the limits identified in quality plan)
- **D** (Sensor drop-out)
- N (No model fit)
- **U** (Unsealed road)

Road works (W) refers side tracks and other road construction which may affect the TSD measurements. S refers to cases when TSD operates outside the speed. Sensor drop-out (D) occurs Sensor drop-out (D) when the doppler lasers give z zero, negligible or negative deflection velocity. The TSD reports deflection bowl from two models, namely the ARRB AUTC model and the Greenwood model. Depending the model fitting outcome, deflection bowl may not be generated, and the system will report an event code of (N).

7 Operational Limitations

The intent of the TSD testing programme is to collect as much of the sealed road network within the allocated time in each state. However, due to the constraints of the vehicle some sections of the sealed network are not able to be tested. These include:

- Sections where manoeuvrability issues which prevent the vehicle being turned around
- Isolated seals (the equipment might be damaged by travelling across unsealed road to access these)
- Roads with significant horizontal curvature or gradient which result in a speed of less than 50 km/hr
- Sections of extreme roughness which could result in a highly variable load applied to the
 pavement surface (reduce the reliability of measurements) and potentially damage the
 equipment
- · Roads where low bridge mass limits prevent passage of the vehicle
- High strength / rigid pavements (where the vertical velocity of the pavement is below the threshold which can be reliably detected by the Doppler lasers)

In addition to the above constraints, the Doppler lasers are only fitted on the left wheelpath of the TSD and generally only the lane specified in the Data Collection Performance Agreement (DCPA), the most heavily trafficked, typically the left most lane, is tested. However, multiple lanes of some roads have been carried out following local requests.

It should also be noted that, like traditional profilometry lasers, Doppler lasers do not operate reliably where the surface of the pavement is moist. For this reason, deployment of TSD equipment in Queensland tends to coincide with drier weather.

The TSD equipment is available for limited project-level testing, provided that TMR Strategic Asset Management (TSAM) receives sufficient notice to schedule the work with the state-wide collection. The proposed testing programme for the TSD is distributed to TMR Districts with a request for feedback or additional sites for testing.

Although the TSD equipment is capable of measuring at sub metre chainage intervals, measurements are currently reported at a minimum interval of ten metres. The velocities or deflections reported for each interval are the mean of sub-metre measurements throughout the interval. The reported chainage is that at the end of each interval in the direction of travel.

8 Analysis Procedures

Figure 3 shows three levels of analysis that can be performed using the TSD deflection data.

Level 1 is the simplest and only utilise the maximum TSD deflection (deflection at 0 mm offset, which is the deflection computed from the AUTC model at the location in the middle of the dual rear tyre). By adopting the TSD-FWD conversion relationship, the TSD can be converted to FWD deflections and used in subsequent analysis. Several conversion relationships have been presented in the past by Austroads (Roberts et al. 2014) and other researchers (Manoharan et al. 2017) in Australia. As there is no universally accepted relationship, the practitioner may adopt the interim relationships presented in Section 10. It is recommended that site specific (FWD-TSD) correlations should be established for the data conversion. (Note: these relationships are expected to be refined in the future as more comparison data becomes available).

Level 2 involves utilising part of full deflection basin from the TSD deflection. Recent research (Lee et al, 2016) in Queensland raised concerns as to whether linear regression is adequate to represent the relationship between TSD and FWD measurements when the offset is beyond 450 mm from the loading point. It was found that the coefficient of determination (R²) drops off rapidly as shown in Figure 5c.

Therefore, in the interim, it is suggested that deflection basin parameters that utilise TSD measurements between 0 to 450 mm offset be adopted. Some of the deflection parameters that satisfy this condition are:

- Curvature (D0 D200)
- Deflection Ratio (D250 / D0)

In the USA, Nasimifar et al. (2018) found TSD measured slopes exhibiting significant noise or anomalies with the slope measurements associated with one or more sensors collected at Virginia I64. The study showed that the presence of anomalous slope measurements in one or more sensors can lead to significant differences in the computed deflections.

In another study conducted at Griffith University (Chai et al. 2016) on Queensland road network, it was observed that most of the pavement sections show nonlinear subgrade behaviour by interpreting the TSD deflection data. The methods to determine the subgrade nonlinearity in pavements are explained in (Ullidtz, 1998) & (Chai et al. 2015). The relatively small velocity slopes at the offset of 600 and 900 mm, and the corresponding D600 and D900 may be linked to inherent nonlinear subgrade behaviour in granular pavements with a relatively thin bituminous layer.

The study has also identified another contributing factor for the small recorded deflection at increasing offset. This may be due to the dynamic effects generated by the TSD axle load on the granular pavements. The deflection bowls show that the radius of influence zone for the granular pavements (with bituminous layer less than 50 mm) is confined within the distance from the load position to the offset of about 450 mm. The small deflections recorded at D600 and D900 are likely caused by the dynamic effect of the TSD load which influences mainly the pavement materials near the impact load at the time of contact.

Therefore, the two contributing factors likely to cause the rapid decrease in the coefficient of determination (R²) when the offset is beyond 450 mm are:

- · subgrade nonlinearity behaviour, and
- the dynamic effects of the TSD axle load.

As such, the low computed D900 deflection to be adopted in the back-calculation should be used with caution, as it can lead to unreasonably high back-calculated subgrade CBR value. The back-calculated subgrade CBR value should be validated using laboratory soaked CBR test and the dynamic cone penetrometer field test. Moderation of the subgrade CBR should also be carried out in accordance with the guideline given in TMR Pavement Rehabilitation Manual (TMR, 2012).

Level 3 involves the process of back-calculating layer moduli using either the TSD surface vertical velocity (Nasimifar et. al. 2017) or the TSD surface deflection using AUTC model as shown in Figure 3. Section 11 describes the methodology presented by the FHWA research group (Nasimifar et. al. 2017). There is limited experience using this approach, and the results should be treated with caution until the accuracy of the method can be verified independently. Engineering judgement should be exercised when interpreting the back-calculated results. At this time, it should not be used beyond network-level assessment.

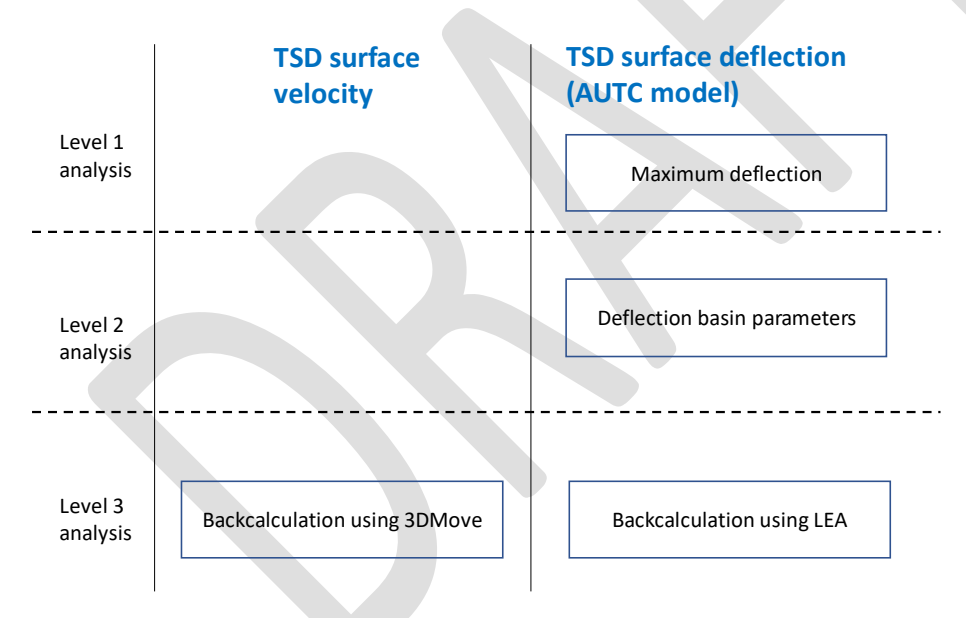
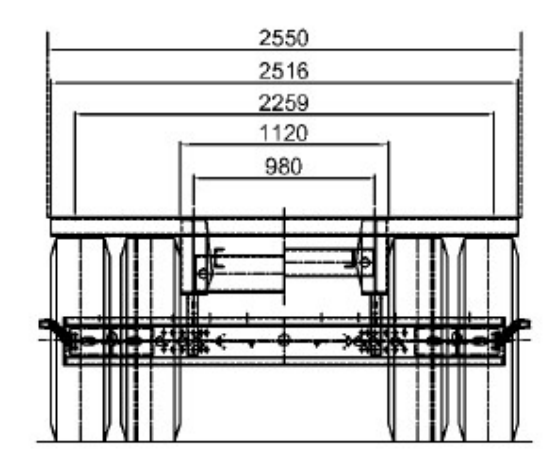


Figure 3 Analysis Procedure using TSD data

9 Modelling the Pavement Surface Response

Whether a traditional static load model such as that employed by CIRCLY (Mincad, 2017) or a dynamic load model such as that used by 3D-Move (3D-Move, 2013) are employed to estimate the surface response, the configuration of the relevant TSD load will need to be considered. Figure 4 illustrates some of the device configuration parameters that will need to be known.



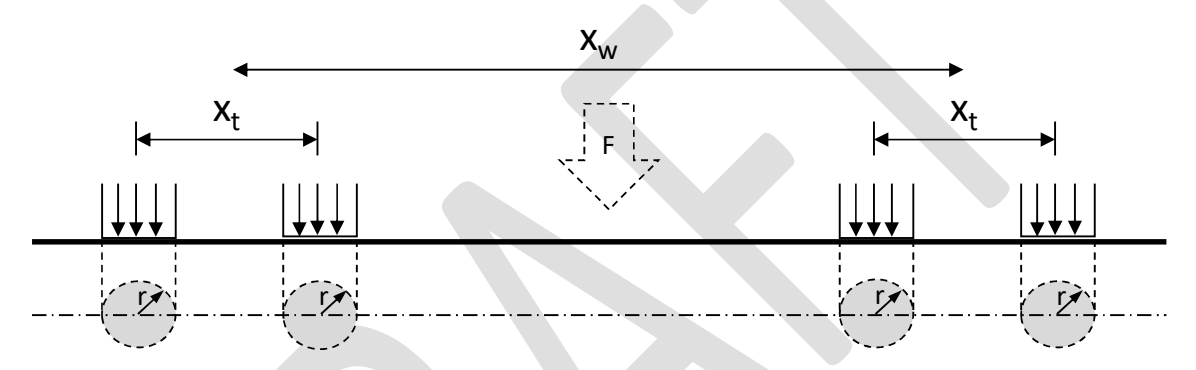


Figure 4 TSD Axle Configuration

where

F = force applied to the axle = 98.1 ± 0.98 kN (refer Table 4)

Xw = the distance between the centre of the wheels = 1800 mm

Xt = the distance between the centre of the tyres = 345 mm

r = the tyre contact radius = 102 mm

Information on the TSD rear axle and tyre configuration is important when one wants to model the pavement response from a TSD. At the current stage, the information from the strain-gauge based load cell are recorded but not currently used to adjust the deflection measurement.

Table 4 TSD loading axle and tyre information

Axle Weight	10.0 ± 0.10 tonne
Axle Force	98.1 ± 0.98 kN
Tyre model	275/70R 22.5
Tyre pressure	760 ± 20 kPa

Source: Austroads AG:AM-T017 (Austroads, 2016b)

The TSD measures the pavement response ahead of the rear wheel of the Intelligent Pavement Assessment Vehicle (iPave) vehicle platform. Measurements are taken at offsets of 100, 200, 300, 450, 600 and 900 mm from the centre of the wheel (Austroads, 2016b)

It will be noted that the traditional measurement at the centre of the load cannot be accommodated because the wheel hub separator prevents the Doppler laser beam from reaching the pavement. (Murnane & Wix, R., 20YR). Instead the measurement at the centre of load, where reported, is estimated from measurements at adjacent offsets.

The tyre model is 275/70R 22.5 (Austroads, 2016b) which indicates a tyre section width of 275 mm, a sidewall height 70% of the section width and wheel rim diameter of 571.5 mm (22.5 inches). The R indicates radial ply construction.

10 Relationship Between TSD and FWD Measurements

The interim relationships between TSD and FWD measurements for the different pavement types are listed in Table 5. These relationships are expected to be refined in the future as more comparison data becomes available. The DR_{FWD} and DR_{TSD} relationship for Deflection Ratio (D250/D0) is given in Table 6.

Similar comparisons of the deflection measured at different offsets from the load were carried out. The slope, intercept and the coefficient of determination (R²) from the linear regression analysis are shown in Table 7 and in Figure 5.

Table 5 Relationship between Maximum Deflections (Lee & Conaghan, 2016)

Pavement Type	Maximum Deflection (D0, mm)	Correlation (R ²)
Non-specific	$D0_{FWD} = 0.900 D0_{TSD} + 0.138$	0.70
Seal over Cement Treated Base (CTB)	$D0_{FWD} = 0.8634 D0_{TSD} + 0.2246$	0.59
Asphalt over Granular	$D0_{FWD} = 0.6509 D0_{TSD} + 0.2176$	0.52
Seal over Granular	$D0_{FWD} = 0.6439 D0_{TSD} + 0.2051$	0.40

Table 6 Relationship between Deflection Ratio (Lee & Conaghan, 2016)

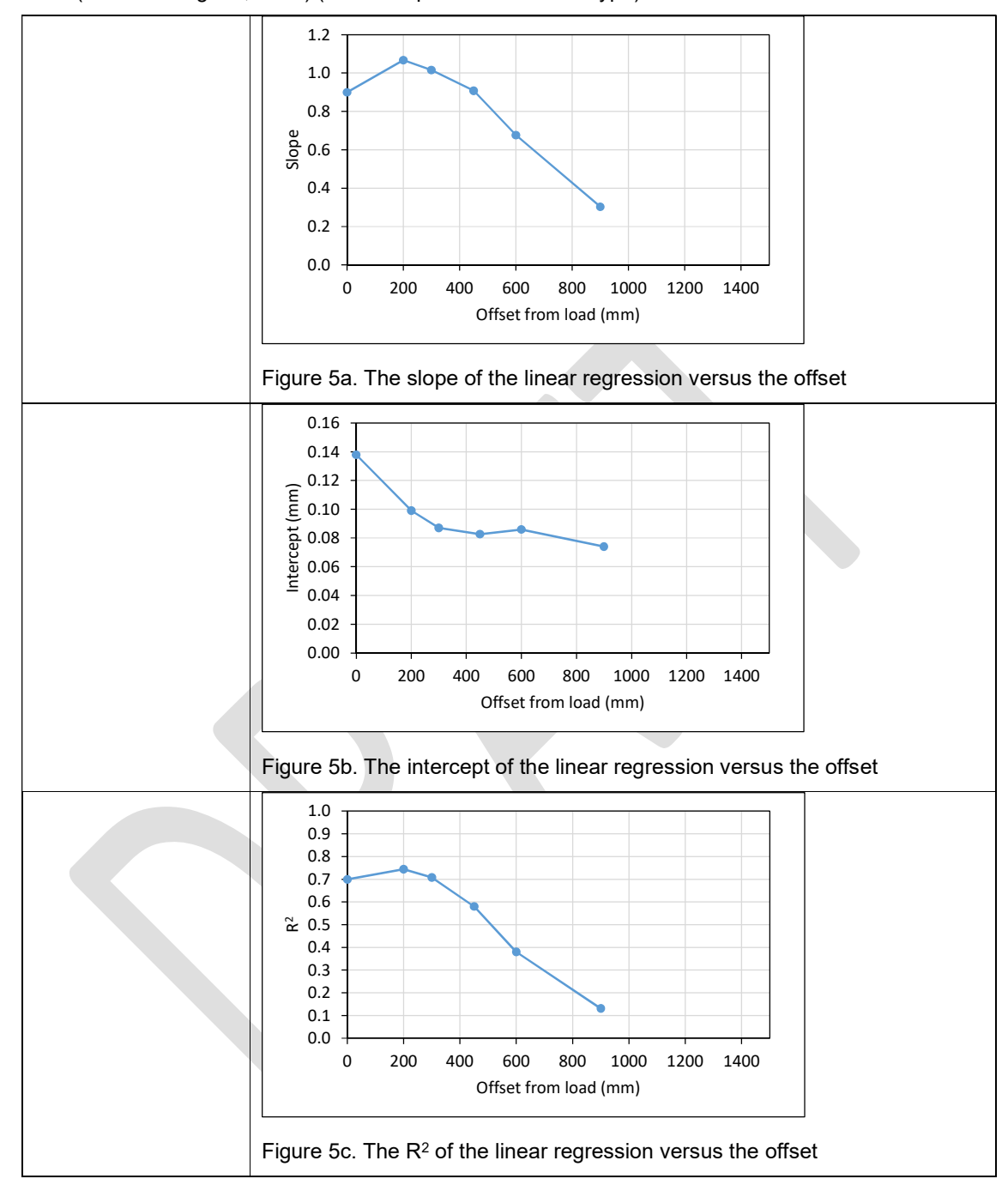
Pavement Type	Deflection Ratio (D250 / D0)	Correlation (R ²)
Non-specific	$DR_{FWD} = 0.530 DR_{TSD} + 0.368$	0.52

Table 7 FWD-TSD Relationships for deflection at D0, D200, D300, D450, D600 & D900 (Lee & Conaghan, 2016) (for Non-Specific Pavement Type)

Sensor Location	Maximum Deflection (D0, mm)	Correlation (R ²)
D0	$D0_{FWD} = 0.900 D0_{TSD} + 0.138$	0.70
D200	$D0_{FWD} = 1.068 D0_{TSD} + 0.0099$	0.74
D300	$D0_{FWD} = 1.016 D0_{TSD} + 0.087$	0.71
D450	$D0_{FWD} = 0.908 D0_{TSD} + 0.083$	0.58
D600	$D0_{FWD} = 0.677 D0_{TSD} + 0.086$	0.38
D900	$D0_{FWD} = 0.303D0_{TSD} + 0.074$	0.13



Figure 5. Linear Regression Results for D0, D200, D300, D450, D600 & D900 measured by TSD and FWD (Lee & Conaghan, 2016) (for Non-Specific Pavement Type)



However, while it has been demonstrated that an approximate relationship exists between the deflection measurements of the TSD and FWD to approximately 300 mm from the centre of load, this relationship degrades for larger offsets (Lee & Conaghan, 2016). The possible causes of the poor (FWD-TSD) correlation at increasing offsets have been explained in Section 8.

11 Back-Calculation Procedure

Forward calculation involves estimating the pavement surface response based on the properties of layers within the pavement. Software such as CIRCLY (MINCAD, 2017) has traditionally been employed to carry out this task assuming a static load.

Back-calculation, as its name implies, attempts to reverse the forward calculation, estimating layer properties, such as the elastic modulus, from the surface response of the pavement.

At the time of writing no software had been developed to back-calculate TSD deflection measurements directly.

However, it is possible to convert TSD deflection measurements to near equivalent FWD measurements, back-calculation software developed for the FWD device could be employed to back-calculate TSD measurements.

Recent research conducted in the United States (Nasimifar et. al 2017) presented two methods, namely the Velocity-Based and the Deflection-Based approaches to estimate the layer moduli for network-level analysis using the TSD. The two approaches, summarised in Table 8, were presented to obtain the back-calculated moduli, and it was concluded that the deflection method provides comparable back-calculated layer moduli with that of velocity method. Thus, the deflection method can be reasonably be used for network level applications until velocity method becomes computationally practical.

Table 8 Back-calculation using the Velocity and Deflection Methods (Nasimifar et. al 2017)

Methods	Steps Outline	
Velocity-Based	Obtain TSD-measured vertical deflection velocities (Vv).	
	Select an analytical software (e.g. 3D-Move) which can simulate TSD dynamic loading characteristics.	
	 Use TSD loading information (refer Section 9 for TSD loading configurations) as input data. 	
	 Trial-and-error to derive a set of layer moduli by matching the modelled and measured TSD velocities, until the root mean square error (RMSE) are minimised. 	
Deflection-Based	Obtain TSD-measured deflection basin (Note 1).	
	Select a back-calculation software that utilises layer elastic. analysis (LEA) algorithm to model the static responses.	
	 Use TSD loading information (refer Section 9 for TSD loading configurations) as input data. In the LEA algorithm, the modelling would be similar to a FWD loading, except that two circular loading areas are used to represent the TSD. 	
	Perform back-calculation as usual using the batching function in the selected back-calculation software.	

Note 1: Nasimifar et. al (2017) used the deflection generated by the Greenwood Engineering model.

The key differences between the two methods are the computation time and the accuracy. In general, analytical software that simulate dynamic loading takes a considerably longer processing time and often lacks batching function to automate the trial-and-error process. However, the study has shown that the velocity-based approach when analysed using 3D-Move software generate the best fitting results with field measurements. Specifically, 3D-Move tends to provide the best fit for pavement structures containing a significant thickness of dynamically-dependent material (e.g. pavement including thick asphalt layers).

As the deflection computed in Australia uses the ARRB AUTC model, it is suggested that the deflection from the AUTC model is used. The TMR back-calculation procedure is shown in Table 9.

Table 9 TMR Back-calculation procedure using Deflection-based Method

Methods	Steps Outline	
Deflection-Based	Obtain TSD-measured deflection basin generated by ARRB AUTC model.	
	 Plot cumulative sum graphs for TSD and FWD deflection (D₀) data across the entire length of the project to delineate homogeneous sections of the pavement condition. 	
	 Establish site specific (TSD - FWD) correlations and compute the equivalent FWD deflections. 	
	Select back-calculation software (e.g. EfromD3) that utilises layer elastic analysis (LEA) algorithm to model the static responses.	
	 Once all the deflections have been converted to FWD, perform back-calculation as usual using the batching function in the selected back-calculation software. 	
	Back-calculation process should be performed in accordance with TMR Pavement Rehabilitation Manual (TMR PRM, 2012).	
	7. The back-calculated pavement layer moduli should be moderated using the (TMR PRM, 2012) manual. In addition, the back-calculated subgrade CBR should be moderated and validated with the laboratory soaked CBR test and dynamic cone penetrometer's inferred CBR value.	

Note 1: TMR uses the deflection generated by ARRB AUTC model.

The framework outlined in the technical note provides a way for practitioner to estimate back-calculated moduli from the TSD data, however, the experience used in Australian projects are very limited, and the results should be treated with caution until the accuracy of the results can be verified independently. Engineering judgement should be exercised when interpreting the back-calculated results. When the converted TSD deflection data is used in the back-calculation, the results should be validated with that obtained from FWD.

12 References

Austroads (2005), RoadFacts: An Overview of the Australian and New Zealand Road Systems, Austroads, Sydney, New South Wales, Australia.

Austroads (2014), Traffic Speed Deflectometer: Data Analysis Approaches in Europe and USA Compared with ARRB Analysis Approach, AP-T280-14 Austroads.

Austroads (2016a), Specification for Pavement Deflection Measurement with a Traffic Speed Deflectometer (TSD) Device, AGAM-S006-16, Austroads.

Austroads (2016b), Pavement Data Collection with a Traffic Speed Deflectometer (TSD) Device, AGAM-T017-16 Austroads.

Baltzer, S., Pratt, D., Weligamage, J., Adamsen, J., Hildebrand, G., (2010), Continuous bearing capacity profile of 18,000 km Australian road network in five months, 24th ARRB Conference. Melbourne, Victoria, 10 pp.

Chai, G., Kelly, G., Huang, A., Chowdhury, S.H., Manoharan, S & Golding, A., (2015), New Approaches for Modelling Non-linearity of Subgrade in asphalt pavements, Presentation at the 94th Transportation Research Board Annual Meeting, Washington D.C., 2015.

Chai, G., Manoharan, S., Golding, A., Kelly, G., Chowdhury, S.H., (2016), Evaluation of the Traffic Speed Deflectometer data using Simplified Deflection Model, Transport Research Procedia 14, Elsevier B.V., 2016.

Kelly, J., & Moffatt, M. (2012), Review of the Traffic Speed Deflectograph – Final Project Report, AP-R395-12 Austroads.

Lee, J., & Conaghan, A. (2016), Benefits of Traffic Speed Deflectometer Data in Pavement Analysis (TSD and FWD) correlation study and investigation to "ground truth" instrumentation, Year 2 – 2015/2016, Project No: 010554, National Asset Centre of Excellence, Queensland Department of Transport.

Manoharan, S. Chai, G., Chowdhury S.H., Golding A., (2017), Prediction of Remaining Structural Service Life using Traffic Speed Deflectometer, World Conference on Pavement and Asset Management (WCPAM), Milan, Italy.

Martin, T. (2012), Benefits and Risks of Investing in Network Level Deflection Data Collection, AP-T217-12 Austroads

Mincad, CIRCLY7 for Mechanistic Pavement Design and Analysis, Mincad Systems Pty Ltd, 383 Church Street, Richmond, Victoria (https://www.mincad.com.au/).

Moffatt, M., & Martin, T. (2013), State-of-the-Art Traffic Speed Deflectometer Practice, AP-T246-13 Austroads

Muller, WB., & Roberts, J. (2013). Revised Approach to Assessing Traffic Speed Deflectometer Data And Field Validation Of Deflection Bowl Predictions. International Journal of Pavement Engineering 14, 388-402.

Murnane, C., Wix., R., & Triplow, C., (2017), Project Quality Manual, Traffic Speed Deflectometer Operations, New Zealand & Australia.

Murnane, C., & Wix R. (20YR), Trials and Tribulations of Traffic Speed Deflectometer Operations, ARRB.

Pedersen, L. (2012), Viscoelastic Modeling of Road Deflections for Use with the Traffic Speed Deflectometer. PhD study in collaboration with Greenwood Engineering, Technical University of Denmark and the Ministry of Science and Innovation, 2012.

Nasimifar, M., R. V. Siddhartha, G. Rada, and S. Nazarian. (2016), Validation of Dynamic Simulation of Slow Moving Surface Deflection Measurements. In Transportation Research Record: Journal of the Transportation Research Board. Transportation Research Board of the National Academies, Washington. D.C., 2016.

Nasimifar, M., Thyagarajan, S., & Sivaneswaran, N. (2017), Backcalculation of Flexible Pavement Layer Moduli from Traffic Speed Deflectometer data, Transportation Research Record 2641: Journal of the Transportation Research Board. Transportation Research Board of the National Academies, Washington. D.C., 2017.

Nasimifar, M., Thyagarajan, S., & Sivaneswaran, N. (2018), Computation of Pavement Vertical Surface Deflections from Traffic Speed Deflectometer Data: Evaluation of Current Methods, Journal of Transportation Engineering, Part B: Pavements, ASCE, 2018.

Rasmussen, S., Aagaard, L., Baltzer, S., Krarup, J. (2008), A Comparison of two Years of Network Level Measurements with the Traffic Speed Deflectometer, 2nd European Transport Research Arena, Ljubljana, 2008.

Robert, J., Ai, U., Toole, T., & Martin, T. (2014), Traffic Speed Deflectometer: Data Review and Lessons Learnt, AP-T279-14 Austroads.

Robert, J., & Byrne, M. (2008), An initial review of the Greenwood Traffic Speed Deflectometer (TSD) and its potential applicability for the RTA, ARRB contract report RC73952, ARRB Group, Vermont South, Victora.

3D-Move. (2013), 3D-Move Analysis Software (Version 2.1) Release Date: June 2013 University of Nevada, Reno (http://www.arc.unr.edu/Software.html)

TMR, (2012), Pavement Rehabilitation Manual, Queensland Department of Main Roads, April 2012.

Ullidtz, P. (1998), Modelling Flexible Pavement Response and Performance, Narayana Press, Gylling, Denmark, 1998.